

1 **Composition and sources of sedimentary organic matter in the deep Eastern**
2 **Mediterranean Sea**

3

4 R. Pedrosa-Pàmies^{1,2}, C. Parinos², A. Sanchez-Vidal¹, A. Gogou², A. Calafat¹, M.
5 Canals¹, I. Bouloubassi³, N. Lampadariou⁴

6

7

8 [1] GRC Geociències Marines, Departament d'Estratigrafia, Paleontologia i
9 Geociències Marines, Universitat de Barcelona. Barcelona, Catalonia.

10 [2] Hellenic Centre for Marine Research (HCMR), Institute of Oceanography.
11 Anavyssos, Attiki, Greece.

12 [3] Laboratoire d'Océanographie et du Climat: Expérimentation et Approches
13 Numériques (LOCEAN), CNRS – Université Pierre et Marie Curie. Paris, France.

14 [4] Hellenic Centre for Marine Research (HCMR), Institute of Oceanography,
15 Heraklion, Crete, Greece.

16

17

18 Correspondence to: A. Sanchez-Vidal (anna.sanchez@ub.edu) Tel: +34934021382;
19 Fax: +34934021340.

20

21 **Abstract**

22 Surface sediments collected from deep slopes and basins (1018-4087 m depth) of
23 the oligotrophic Eastern Mediterranean Sea have been analysed for bulk elemental
24 and isotopic composition of organic carbon, total nitrogen and selected lipid
25 biomarkers, jointly with grain size distribution and other geochemical proxies. The
26 distribution and sources of sedimentary organic matter (OM) have been subsequently
27 assessed and general environmental variables, such as water column depth and
28 physical circulation patterns, have been examined as causative factors of deep-sea
29 sediment characteristics. Lithogenic and biogenic carbonates are the dominant
30 sedimentary fractions, accounting for up to 85.4% and 66.5% of the total weight,
31 respectively. The low OC and TN contents in the surface sediments of the study
32 area, that ranged from 0.15 to 1.15% and 0.06 to 0.11%, respectively, reflect the
33 oligotrophic character of the EMS. Both bulk and molecular organic tracers reflect a
34 mixed contribution from autochthonous and allochthonous sources for the
35 sedimentary OM, as indicated by relatively degraded marine OM, terrestrial plant
36 waxes and anthropogenic OM e.g., degraded petroleum by-products, respectively.
37 Wide regional variations have been observed amongst the studied proxies, which
38 reflect the multiple factors controlling sedimentation in the deep Eastern
39 Mediterranean Sea. Our findings highlight the role of deep Eastern Mediterranean
40 basins as depocentres of organic-rich fine-grained sediments (mean $5.4 \pm 2.4 \mu\text{m}$),
41 with OM accumulation and burial being attributed to aggregation mechanisms and
42 hydrodynamic sorting. A multi-proxy approach is applied aiming to investigate the
43 biogeochemical composition of sediment samples, which sheds new light on the
44 sources and transport mechanisms along with the impact of preservation vs.
45 diagenetic processes on the composition of sedimentary OM in the deep basins of
46 the oligotrophic Eastern Mediterranean Sea.

47

48 1 Introduction

49 The burial of organic matter (OM) in marine sediments constitutes the main link
50 between "active" pools of carbon in the oceans, atmosphere and landmasses, and
51 carbon pools that cycle on much longer, geological, time scales (Burdige, 2007).
52 Therefore, investigating the processes that control the composition of sedimentary
53 OM that is buried in deep-sea sediments is crucial for understanding carbon cycling
54 on a global scale.

55 The deep sea receives inputs of organic particles from multiple sources, both
56 autochthonous (e.g., biogenic particulate matter from primary production in ocean
57 surface waters) and allochthonous (i.e. land-sourced OM from soils, plant debris,
58 riverine phytoplankton and man-made compounds transported by runoff and
59 atmospheric deposition into the marine domain) (Bouloubassi et al., 1997; Durrieu de
60 Madron et al., 2000; Kaiser et al., 2014). Consequently, sedimentary OM constitutes
61 an heterogeneous and complex mixture of organic compounds with a wide range of
62 chemical and physical properties (Mayer, 1994; Hedges and Oades, 1997; Hedges et
63 al., 1997; Goñi et al., 1998). Therefore, the combined use of bulk geochemical
64 indicators such as total nitrogen (TN) to organic carbon (OC) ratios, stable isotope of
65 OC ($\delta^{13}\text{C}$), and molecular proxies such as lipid biomarkers can aid to gain knowledge
66 on the origin, delivery and preservation of OM in marine sediments (Bouloubassi et
67 al., 1997; Meyers, 1997; Goñi et al., 2003; Volkman, 2006).

68 The biogeochemical composition of sediments in deep basins of the oligotrophic
69 Eastern Mediterranean Sea (EMS), as well as the sources, transport and
70 preservation of sedimentary OM, have been scarcely investigated so far. Previous
71 studies have shown that the composition of surficial sediments is principally
72 controlled by the geochemical characteristics of the source areas, the prevailing
73 metoceanic conditions on the adjacent shelves, the contribution of atmospheric
74 aerosols and the dominant regional circulation (e.g., Weldeab et al., 2002; Ehrmann
75 et al., 2007; Hamann et al., 2008). Nevertheless, the factors involved in the supply,
76 distribution and fate of sedimentary OM are still poorly known.

77 In the present study, surface sediments collected from deep slopes and basins of the
78 EMS have been analysed for physical and geochemical parameters such as grain
79 size distribution, lithogenic, calcium carbonate (CaCO_3), opal, OC and TN contents,

80 along with molar TN/OC ratios, stable isotopic ratios of OC ($\delta^{13}\text{C}$) and selected lipid
81 biomarkers. Our main goal is to investigate the spatial distribution and main sources
82 of sedimentary OM and to evaluate the impact of autochthonous vs. allochthonous
83 contributions in the study area. We also examine whether and up to which point
84 general environmental factors, such as water mass circulation patterns and water
85 column depth, could explain the observed deep-sea sediment geochemical
86 properties.

87

88 **2 Oceanographic setting**

89 The EMS is a land-locked sea with a complex topography including shelves, slopes,
90 ridges, seamounts, trenches and four main basins: the Adriatic Sea, the Ionian Sea,
91 the Aegean Sea and the Levantine Sea (Fig. 1) (Amblàs et al., 2004; Medimap
92 Group, 2007). The Ionian Sea to the west and the Levantine Sea to the east are
93 longitudinally connected and cover most of the EMS area. They are also the deepest
94 basins of the EMS, with the maximum depth (5267 m) located at the Hellenic Trench,
95 south of the Cretan Arc. The Aegean Sea and the Adriatic Sea represent the
96 northern extensions of the EMS. Both are relatively shallow, in particular the Adriatic
97 Sea, which is dominated by a broad shelf and a slope sub-basin shallower than 1200
98 m. In the Aegean Sea, which has a particularly complex topography with tens of
99 depressions, highs and islands, water depths up to 2500 m are found north of the
100 island of Crete (Amblàs et al., 2004; Medimap Group, 2007). The southern Aegean
101 Sea (Cretan Sea) is the sea area comprised between the Cyclades Archipelago to
102 the north and the island of Crete to the south, which also includes the western Cretan
103 Straits.

104 The general circulation pattern of the EMS is anti-estuarine, which results from
105 interactions between basin, sub-basin and mesoscale flows (Bethoux, 1979). The
106 EMS communicates with the Western Mediterranean Sea through the Sicily Strait,
107 with an inflow of low-salinity Modified Atlantic Water (MAW) at the upper 100-150 m
108 of the water column (Rabitti et al., 1994; Malanotte-Rizzoli et al., 1997). MAW flows
109 in an easterly direction getting progressively saltier and warmer till transforming into

110 Levantine Intermediate Water (LIW) into the Levantine Sea where it sinks to mid
111 depths (Milliff and Robinson, 1992; Lascaratos et al., 1993).

112 The Eastern Mediterranean Deep Water (EMDW) is a relatively well oxygenated
113 water mass, likely as a result of the formation and sinking of warm deep-water that
114 ventilates the deepest levels in the EMS (Schlitzer et al., 1991; Roether and Well,
115 2001; Meador et al., 2010). Waters from the Adriatic Sea (Adriatic Deep Waters,
116 ADW) have been considered as the main contributor of deep and bottom waters to
117 the EMS (Malanotte-Rizzoli and Hecht, 1988). Nevertheless, the Aegean Sea
118 constitutes a sporadically significant contributor to EMDW through the Cretan Deep
119 Water (CDW), as in the case of the Eastern Mediterranean Transient (EMT) anomaly
120 in the 1990s (Lascaratos et al., 1999; Theocharis et al., 1999). Additionally, the
121 Aegean Sea constitutes a possible secondary source of intermediate waters to the
122 adjacent Ionian and Levantine seas, through outflows across the Cretan Arc straits
123 (Robinson et al., 2001).

124 Key factors that control the exchanges through the Cretan Arc straits are the
125 thermohaline properties of water masses and mesoscale variability. For example, the
126 Ierapetra anticyclonic gyre, which is located off the southeast corner of Crete
127 (Ierapetra Basin), exhibits a strong seasonal signal that is linked to variations of the
128 outflow across the eastern Cretan Arc straits (Theocharis et al., 1993; Larnicol et al.,
129 2002). Actually, the several permanent and/or recurrent eddies in each of the EMS
130 sub-basins enhance exchanges between continental shelf and slope waters
131 (Robinson et al., 1992; Malanotte-Rizzoli et al., 1997; Millot and Taupier-Letage,
132 2005), which in turn influence primary productivity and the settling of OM to the deep-
133 sea floor (Danovaro et al., 2010).

134 Thermohaline circulation and overall environmental conditions make the EMS one of
135 the most ultra-oligotrophic environments of the world ocean (Psarra et al., 2000;
136 Krom et al., 2005; Thingstad et al., 2005; Gogou et al., 2014a). Annual primary
137 production in the EMS averages between 121 and 145 g C m⁻² y⁻¹ (Bosc et al., 2004;
138 Gogou et al., 2014b). However, the fraction of primary production exported below
139 2000 m of water depth averaged 0.3% (Gogou et al., 2014b). The low autochthonous
140 contribution to OM fluxes in the deep open EMS is counterbalanced by allochthonous
141 inputs resulting from long-range atmospheric transport and deposition by aerial dust

142 (Jickells, 1995; Gogou et al., 1996; Tsapakis and Stephanou, 2005). The overall
143 sedimentation rate in the deep areas of the open EMS is low (i.e. 2-5 cm kyr⁻¹) (Van
144 Santvoort et al., 1996, 2002; Garcia-Orellana et al., 2009; Stavrakakis et al., 2013).

145

146 **3 Materials and methods**

147 **3.1 Sampling**

148 Short sediment cores were collected with a multicorer at 29 stations, ranging from
149 1018 to 4087 m water depth, during six oceanographic cruises in the Ionian Sea, the
150 southern Aegean Sea (Cretan Sea) and the northwestern Levantine Sea from
151 January 2007 to June 2012 (Fig. 1 and Table 1). Once onboard, multicores were
152 visually described and sliced at 1-cm intervals. Sub-samples collected for grain size,
153 elemental and stable isotopic composition were stored in sealed plastic bags at 4°C,
154 while those collected for the analysis of lipid biomarkers were stored in pre-
155 combusted aluminium foils at -20°C. Only the undisturbed top centimetre of each
156 sediment core is considered in this study.

157

158 **3.2 Analytical procedures**

159 **3.2.1 Particle size characterization**

160 The grain size distribution of sediment samples was determined using a Coulter
161 LS230 Laser Diffraction Particle Size Analyzer, which measures sizes between 0.04
162 and 2000 µm. Prior to analysis, freeze-dried samples were oxidized with a 10% H₂O₂
163 (v/v) solution in order to remove OM. Each sample was then divided into two sub-
164 samples, one of which was treated with 1M HCl to remove carbonates and thus
165 obtain the grain size distribution of lithogenic (siliciclastic) particles. Subsequently,
166 both bulk and lithogenic fractions were dispersed into 20 cm³ of a 5% NaPO₅ (v/v)
167 solution and mechanically shaken for 4 hours, and then introduced into the particle
168 size analyzer after using a 2000 µm sieve to retain occasional coarse particles that
169 might obstruct the flow circuit of the instrument.

170 The measured particle size spectrum is presented as % volume in a logarithmic
171 scale, where volume is calculated from particle diameter, assuming spherical shapes.

172 Results were recalculated to percentages of clay (<4 μm), silt (4-63 μm) and sand
173 (63 μm -2 mm).

174

175 **3.2.2 Elemental and stable isotopic analysis of carbon and nitrogen**

176 For the determination of total carbon (TC), TN, OC contents and stable isotopic
177 composition of OC ($\delta^{13}\text{C}$) freeze-dried and ground sediments were analysed using a
178 Flash 1112 EA elemental analyser interfaced to a Delta C Finnigan MAT isotope ratio
179 mass spectrometer. Samples analyzed for %OC and $\delta^{13}\text{C}$ were initially de-
180 carbonated using repetitive additions of a 25% HCl (v/v) solution, separated by 60°C
181 drying steps, until no effervescence was observed (Nieuwenhuize et al., 1994).
182 Stable isotope data are reported using the conventional per thousand $\delta^{13}\text{C}$ notation
183 relative to the Pee Dee Belemnite standard. Uncertainties for elemental composition
184 were lower than 0.1%, while uncertainty for $\delta^{13}\text{C}$ was lower than 0.05‰.

185 In consistency with published data in the Mediterranean Sea we assumed OM as
186 twice the OC content (e.g., Heussner et al., 1996; Masqué et al., 2003). The
187 inorganic carbon content was calculated from the difference between TC and OC
188 measurements. Assuming all inorganic carbon is contained within calcium carbonate,
189 CaCO_3 content was determined using the molecular ratio of 100/12.

190 Molar TN/OC ratios were also calculated. TN/OC is plotted in order to constrain the
191 elemental ratios of N-depleted samples (i.e. $\text{TN/OC} \approx 0$ rather than $\text{OC/TN} \infty 0$)
192 following Goñi et al. (2006), and to avoid the underestimation of the terrestrial-
193 derived carbon fraction (Perdue and Koprivnjak, 2007).

194

195 **3.2.3 Biogenic opal and lithogenic fraction analysis**

196 The biogenic silica content was analysed using a two-step 2.5 h extraction with a
197 0.5M Na_2CO_3 solution, separated by centrifugation of the leachates. Si and Al
198 contents of both leachates were analysed with a Perkin-Elmer Optima 3200RL
199 Inductive Coupled Plasma Optical Emission Spectrometer (ICP-OES), correcting the
200 Si content of the first leachate by the Si/Al ratio of the second one. All values are
201 reported as opal ($\text{SiO}_2 \cdot 0.4\text{H}_2\text{O}$), a parameter defined by 2.4 times the weight
202 percentage of biogenic Si content determined for each sample (Mortlock and

203 Froelich, 1989). The opal detection limit, associated to the detection limit of the ICP-
204 OES system, is approximately 0.2%.

205 The lithogenic fraction was estimated by subtracting the concentration of the major
206 constituents from total dry weight (%lithogenic= 100 – [%OM + %CaCO₃ + %opal]).
207 This fraction represents the residual component of particles such as quartz,
208 feldspars, clay minerals and aluminosilicates (Mortlock and Froelich, 1989).

209

210 **3.2.4. Lipid biomarkers analysis and definitions of molecular indices**

211 The analytical procedure followed for the determination of lipid biomarkers has been
212 previously presented in detail (Gogou et al., 1998, 2000, 2007). Briefly, freeze-dried
213 sediment samples were initially solvent-extracted three times by sonication with a
214 dichloromethane: methanol mixture (4:1, v/v). Combined extracts were subsequently
215 separated into different compound classes by column chromatography using silica
216 gel that had been activated for 1 hour at 150 °C. The following solvent systems were
217 used to elute different compound classes: (1) *n*-hexane (fraction F₁, aliphatic
218 hydrocarbons), (2) dichloromethane/*n*-hexane (fraction F₂, carbonyl compounds) and
219 (3) ethyl acetate/*n*-hexane (fraction F₃, alcohols, sterols).

220 F₁ and F₃ fractions were analyzed by Gas Chromatography-Mass Spectrometry (GC-
221 MS) while F₂ fractions were analyzed by Gas Chromatography using Flame
222 Ionization Detection (GC-FID). Hydroxyl-bearing compounds (fraction F₃) were
223 derivatized to the corresponding trimethylsilyl ethers prior to GC-MS analysis using
224 N,O-bis-(trimethylsilyl)-trifluoroacetamide (BSTFA) + 1% trimethylchlorosilane
225 (TMCS) for 1hour at 80°C. Details regarding the GC instrumental parameters are
226 presented elsewhere (Gogou et al., 2007; Parinos et al., 2013).

227 The individual lipids were identified by a combination of comparison of GC-retention
228 times to authentic standards and comparison of their mass spectral data to those in
229 the literature. Quantification was based on the GC-MS or GC-FID response and
230 comparison of peak areas with those of known quantities of standards added prior to
231 the extraction of the sediment samples ([²H₅₀]*n*-tetracosane for *n*-alkanes, *n*-
232 hexatriacontane for long-chain alkenones, 5α-androstan-3β-ol for sterols and
233 heneicosanol for *n*-alkanols). The signal of the Unresolved Complex Mixture (UCM)

234 of aliphatic hydrocarbons was defined by the chromatographic area (fraction F_1)
235 between the solvent baseline and the curve defining the base of resolved peaks.
236 UCM quantification was performed relatively to [$^2\text{H}_{50}$]*n*-tetracosane using the average
237 response factor of *n*-alkanes.

238 Procedural blanks processed in parallel to the samples were found to be free of
239 contamination. Reproducibility of the analytical method based on multiple extractions
240 of sediments was better than 6% in all cases.

241 A range of selected lipid biomarkers are considered in this study, namely long chain
242 *n*-alkanes and *n*-alkanols, long-chain alkenones, long-chain diols & keto-ols and a
243 suite of sterols, along with lipid biomarkers' indices, as proxies of organic matter
244 sources and/or degradation. As OC can vary due to the supply of inorganic material
245 (dilution effect) the concentrations of the reported lipid compounds were normalized
246 to OC contents.

247 The sum of the concentrations of the most abundant high molecular weight *n*-alkanes
248 and *n*-alkanols, which are major components of epicuticular higher plant waxes
249 (Eglinton and Hamilton, 1967; Ohkouchi et al., 1997), are defined, respectively, as:

250

$$251 \quad \sum \text{TerNA} = \sum n\text{-C}_{27,29,31,33} \quad (1)$$

$$252 \quad \sum \text{TerN-OH} = \sum n\text{-C}_{24,26,28,30} \quad (2)$$

253

254 The sum of the concentrations of the considered lipid biomarkers having a clear
255 marine (algal) origin (see Sect. 5.1.2) was calculated as follows:

256

$$257 \quad \sum \text{Mar} = \sum ({}_{28}\Delta^{5,22E} + {}_{30}\Delta^{22E} + \text{C}_{30} \text{ diols \& keto-ols + alkenones}) \quad (3)$$

258

259 The abundance of the Unresolved Complex Mixture (UCM) of aliphatic hydrocarbons,
260 a commonly observed persistent contaminant mixture in marine sediments consisting
261 of branched alicyclic hydrocarbons (Gough and Rowland, 1990), is used as an

262 indicator of the contribution from degraded petroleum products, i.e. chronic oil
263 pollution in the study area (Wang et al., 1999).

264 The Carbon Preference Indices of long chain *n*-alkanes (CPI_{NA}) and *n*-alkanols (CPI_{N-OH})
265 have been used as indicators of terrestrial OM degradation with CPI values in
266 fresh leaves being typically >4 (Collister et al., 1994). However, the abundance of
267 non-degraded petroleum hydrocarbons could potentially bias (lower) CPI_{NA} values
268 with increasing petroleum contribution, since *n*-alkane compounds of petroleum
269 products present CPI_{NA} values ~1 (Wang et al., 1999). The indices were calculated,
270 respectively, as:

271

$$272 \text{ CPI}_{\text{NA}} = \frac{\sum([n\text{-C}_{25}] - [n\text{-C}_{33}])}{\sum([n\text{-C}_{26}] - [n\text{-C}_{34}])} \quad (4)$$

$$273 \text{ CPI}_{\text{N-OH}} = \frac{\sum([n\text{-C}_{24}] - [n\text{-C}_{30}])}{\sum([n\text{-C}_{23}] - [n\text{-C}_{29}])} \quad (5)$$

274

275 Finally, the abundance ratio of $\sum\text{TerNA}$ to $\sum\text{TerN-OH}$ is used as a proxy of the
276 proportion of refractory vs. labile terrestrial components, since $\sum\text{TerNA}$ are more
277 resistant to degradation than their alcohol counterparts (Eglinton and Hamilton, 1967;
278 Ohkouchi et al., 1997). The ratio is defined as:

279

$$280 \frac{[\text{NA}]}{[\text{N-OH}]} = \frac{[\sum\text{TerNA}]}{[\sum\text{TerN-OH}]} \quad (6)$$

281

282 3.2.5 Data analysis and presentation

283 Statistical treatment of grain size data was carried out using the GRADISTAT v. 8.0
284 software (Blott and Pye, 2001). Median diameter (D_{50}), sorting and skewness were
285 calculated geometrically (in metric units) following the approach of Folk and Ward
286 (1957), which is most appropriate when data are non-normally distributed, as in the
287 case of polymodal sediments from the study area.

288 D_{50} was calculated as the average equivalent diameter, which is the diameter where
289 50% of the sediment sample has a larger equivalent diameter and the other 50% has
290 a smaller equivalent diameter. Sorting (expressed by the standard deviation)

291 indicates the fluctuation in the degree of kinetic energy and the depositional regime
292 on grain size characteristics. Skewness measures the degree of asymmetry onto
293 particle distribution. The skewness for a normal distribution is zero, and any
294 symmetric data should have skewness near zero. Positive values indicate skewness
295 towards the finer grain sizes (skewed left) while negative values indicate skewness
296 towards the coarser grain sizes (skewed right). The results of grain size distribution
297 analysis were hierarchically clustered (using IBM SPSS Statistics 18.0) according to
298 the above statistical parameters (autoscaled prior to cluster analysis), in order to
299 determine the similarity of samples within each station measuring the squared
300 Euclidean distance.

301 Principal component analysis (PCA) was performed on standardized grain size and
302 elemental composition data (%clay and sorting of lithogenic and bulk fractions,
303 lithogenic, CaCO₃, OC and TN contents), on standardized bulk organic matter
304 signatures (molar TN/OC ratios and $\delta^{13}\text{C}$) and on standardized indices and mass-
305 normalized concentrations of lipid biomarkers. A subroutine, the Varimax rotation,
306 was applied to the first three factors in order to maximize or minimize loadings within
307 each factor, and thus simplify the visual interpretation of PCA projections. Correlation
308 analysis was also performed using the same variables. In certain occasions during
309 correlation analysis, the singular stations that were clearly out of the trend were
310 excluded in order to strengthen the evident trends of the examined variables. These
311 stations are explained in detail in the discussion section (see Sect. 5.2).

312 The spatial distribution of the various geochemical parameters' contents, bulk OM
313 signatures and selected lipid biomarkers' concentrations/indices considered in this
314 study were visualized using Ocean Data View (ODV) (Schlitzer, 2011).

315

316 **4 Results**

317 **4.1 Grain size characteristics**

318 The grain size composition (% clay, silt and sand) and the sedimentary parameters
319 (D_{50} , sorting and skewness) are presented in Table 2, while the statistical
320 dendrogram, type-averaged grain size spectrum and spatial distributions of grain size
321 types are presented in Figure 2.

322 Silt- and clay-sized particles dominate the bulk sediment, accounting for up to 76.7%
323 and 57.1% of the total weight, respectively (Table 2). The lowest values (<40%) for
324 the silt fraction are found in the upper slope of the western Cretan Straits (station
325 Red3) and the northwestern Levantine Sea (station BF19), while the highest values
326 (>65%) correspond to the Ionian Sea (stations H12 and H03). The lowest clay
327 contents (<20%) are also found in the upper slope of the western Cretan Straits
328 (station Red3) but also in the northeastern Ionian Sea (station H12), while maximum
329 values (>55%) are recorded at the northwestern Levantine Sea (station Red1.1 in
330 Ierapetra Basin) and the western Cretan Straits (station H01). Sand contents show
331 large variations, i.e. from 0 to 47.7% (station Red3 in the upper slope of western
332 Cretan Straits), with values less than 2% in most of the stations (Table 2). Relatively
333 high values (>10%) are also obtained in the northwestern Levantine Sea (stations
334 Red2, BF19 and BF24). D_{50} values range between 3.5 and 56.6 μm (Table 2).

335 Sorting of bulk sediment ranges from 3.0 to 5.2 (Table 2). Most of the northwestern
336 Levantine Sea and western Cretan Straits' stations are very poorly sorted and all
337 stations within the southern Aegean Sea and most of the Ionian Sea are poorly
338 sorted (Table 2 and Fig. 2a). Skewness values for the investigated samples range
339 from -0.45 to 0.27 (Table 2), varying from a very clear negative skewness in the
340 upper slope of the western Cretan Straits (station Red3), to positive skewness in the
341 northwestern Levantine Sea (stations Red2.1, BF19, BF22 and BF24).

342 The hierarchical cluster analysis of all bulk sediment samples resulted into seven
343 grain-size types (Fig. 2a). Most of the samples group into cluster types I (n=11), II
344 (n=6) and III (n=6), with grain size profiles almost symmetrical and poorly sorted, and
345 a dominance of clay and silt fractions. Type V includes three very poorly sorted and
346 positive skewed samples from the northwestern Levantine Sea, which consist mainly
347 of clay and silt fractions. Types IV, VI and VII include only one sample each (Red2,
348 H12 and Red3, respectively). Samples Red2 and Red3, dominated by coarse silt
349 fractions (D_{50} 11.1 μm and 56.61 μm , respectively), are both very poorly sorted but
350 with different types of skewed distributions (symmetrical and negatively skewed,
351 respectively). Finally, sample H12, composed mostly of fine silt, is poorly sorted and
352 slight positive skewness.

353 As in the bulk sediment, silt- and clay-sized particles dominate the lithogenic fraction,
354 accounting for up to 73.5% and 50.8% of the total weight, respectively. The
355 hierarchical cluster analysis of the lithogenic fraction identified six grain size types
356 (clusters) (Fig. 2b). A majority of samples are highly similar (types I-V), with an
357 average composition of $35.2 \pm 5.6\%$ clay, $63.5 \pm 5.3\%$ silt and $1.3 \pm 2.3\%$ sand, a D_{50} of
358 $6.6 \pm 1.3 \mu\text{m}$ and a bimodal or trimodal, symmetrical, poorly sorted grain size
359 distribution. Sample Red3 from the upper slope of western Cretan Straits is an
360 exception, in which belongs to type VI. The composition of its lithogenic fraction is
361 10.3% clay, 34.6% silt and 55.1% sand, with a D_{50} of $78.1 \mu\text{m}$ and a bimodal, very
362 poorly sorted and negatively skewed grain size distribution (Fig. 2b and Table 2).

363

364 **4.2 Bulk geochemical sediment composition**

365 The spatial variability of lithogenics, CaCO_3 , OC and TN contents within the study
366 area is presented in Figure 3a-c.

367 The lithogenics content in the analyzed surface sediments range between 32.5 and
368 85.4% (Fig. 3a). Higher percentages ($>70\%$) are found in stations of the Ionian Sea
369 (with the exception of station H02), while the lowest percentages ($<40\%$) are found in
370 the southern Aegean (stations Red4 and Red5) and northwestern Levantine seas
371 (stations Her01 and BF19) (Table 2). The CaCO_3 contents also show a wide range of
372 values throughout the study area, from 13.2 to 66.5% (Fig. 3b and Table 2). Stations
373 in the western Ionian Sea (H04, BF27, H03, BF15, BF13 and H07) have the lowest
374 CaCO_3 contents ($<22\%$), whereas most stations in the southern Aegean and
375 northwestern Levantine seas and in the western Cretan Straits have elevated CaCO_3
376 contents ($>40\%$).

377 Opal contents are very low, ranging from below detection limits to a maximum of
378 0.24% in the southern Aegean and northwestern Levantine seas (stations Red5 and
379 Red13) (Table 2). Since opal contents are very close to the detection limits, those
380 values can be considered as negligible. Therefore inorganic geochemical fraction of
381 the investigated deep EMS sediments consists only of lithogenic (terrigenous) and
382 carbonate components.

383 OC contents in the studied samples range from 0.15 to 1.15%, with an average value
384 of 0.47% (Table 2). The lowest values are recorded in the northeastern Ionian Sea,
385 south of Otranto Strait (station H12), while the highest values are found off the Gulf of
386 Taranto (station H07), followed by stations in the Ionian Sea (stations BF27, H04 and
387 H03). TN contents range from 0.01 to 0.11% with an average value of 0.06%. TN
388 display a pattern similar to OC, also with the highest values recorded off the Gulf of
389 Taranto (station H07) and the lowest south of Otranto Strait (station H12), both in the
390 northern Ionian Sea.

391

392 **4.3 Elemental and stable isotopic composition of sedimentary OM**

393 The spatial distribution of molar TN/OC ratios and $\delta^{13}\text{C}$ within the study area is
394 presented in Figure 3d-e.

395 Molar TN/OC ratios of the sedimentary OM range from 0.08 to 0.16 (Fig. 3d and
396 Table 2). The highest molar TN/OC ratios values (>0.14) are recorded in the
397 southern Aegean (station Red8) and northwestern Levantine (stations Her01, BF22
398 and BF24) seas, whereas the lowest molar TN/OC ratios (<0.09) are recorded in
399 stations from the northwestern Levantine Sea (station Red15.1), the western Cretan
400 Straits (stations Red3 and Red3.1) and the northern Ionian Sea (stations H07 and
401 H12). However, there is no clear spatial trend (Fig. 3d).

402 The spatial distribution of $\delta^{13}\text{C}$ values shows that relatively lower values are more
403 common in the Ionian Sea than in the northwestern Levantine Sea, the southern
404 Aegean Sea and the south Ionian Sea (Fig. 3e). $\delta^{13}\text{C}$ values range from -18.3 to -
405 24.6‰ (Fig. 3e and Table 2), with stations from the Ionian Sea (stations H03, H07
406 and H12) yielding relatively depleted $\delta^{13}\text{C}$ values ($<-24\text{‰}$) and stations from the
407 western Cretan Straits (station Red3) and the northwestern Levantine Sea (Ierapetra
408 Basin, stations BF22, Red1.1 and Ier01) having relatively enriched $\delta^{13}\text{C}$ values ($>-$
409 22‰).

410

411 4.4 Lipid biomarkers

412 The analysed sedimentary aliphatic hydrocarbons comprise of a series of resolved
413 compounds, mainly *n*-alkanes, and a UCM (Parinos et al., 2013). The UCM dominate
414 amongst aliphatic hydrocarbons in concentrations ranging between 0.50 and 6.64 mg
415 g OC⁻¹ (Fig. 4a and Table 3). Maximum concentrations (>5 mg g OC⁻¹) are recorded
416 in the northwestern Levantine Sea (station Red2.1) followed by the deep central
417 Ionian Sea (station H03). The lowest UCM values (<1.0 mg g OC⁻¹) are obtained in
418 the northern Ionian Sea (station H12) and in the western Cretan Straits (station H01),
419 while rather low values are also recorded in the southern Aegean Sea and west of
420 Crete.

421 The molecular profile of the *n*-alkanes is dominated by long chain homologues ($C_n \geq$
422 24), maximizing at *n*-C₃₁, with elevated CPI_{NA} values (4.9±1.6) (Table 3). Σ TerNA
423 range between 40.8 and 483 $\mu\text{g g OC}^{-1}$, with an average value of 172 $\mu\text{g g OC}^{-1}$ (Fig.
424 4b and Table 3). The station with the highest concentration (station Red2.1) is found
425 in the northwestern Levantine Sea, while the stations with the lowest ones (<110 μg
426 g OC⁻¹) are located in the northern Ionian Sea (stations H07 and H12) and in the
427 southern Aegean Sea (station Red9). Furthermore, relatively elevated Σ TerNA
428 concentrations (>210 $\mu\text{g g OC}^{-1}$) are recorded at the deep station of the western
429 Cretan Straits' (station Red3.1) and the deep central Ionian Sea (stations H03 and
430 H05).

431 The aliphatic alcohol fraction is dominated by a series of *n*-alkanols ranging from *n*-
432 C₂₂ to *n*-C₃₀, with maxima at *n*-C₂₆, and elevated CPI_{N-OH} values (4.5±0.8) (Table 3).
433 Σ TerN-OH range from 13.4 to 105 $\mu\text{g g OC}^{-1}$, with an average of 40.4 $\mu\text{g g OC}^{-1}$,
434 displaying similar distribution with Σ TerNA (Fig. 4c and Table 3). The [NA]/[N-OH]
435 ratios for the analysed sediments range between 2.9 and 6.9, with an average of
436 4.3±0.9 (Table 3).

437 Long-chain di- and tri-unsaturated C₃₇ and C₃₈ methyl ketones and C₃₈ ethyl ketones,
438 commonly referred to as long-chain alkenones, are present in all samples with total
439 concentrations ranging from 3.41 to 30.5 $\mu\text{g g OC}^{-1}$, 13.0 $\mu\text{g g OC}^{-1}$ on average. The
440 major C₂₇-C₃₀ sterols considered in this study, i.e. cholesterol (cholest-5-en-3 β -ol;
441 ₂₇ Δ^5), brassicasterol (24-methylcholesta-5,22-dien-3 β -ol; ₂₈ $\Delta^{5,22}$), β -sitosterol (24-
442 ethylcholesta-5-en-3 β -ol; ₂₉ Δ^5) and dinosterol (4 α ,23,24-trimethyl-5 α (H)-cholest-

443 22(E)-en-3 β -ol -₃₀ Δ ²²), have total concentrations ranging between 10.3 and 62.4 $\mu\text{g g OC}^{-1}$,
444 OC^{-1} , averaging 31.7 $\mu\text{g g OC}^{-1}$. Long-chain C₃₀ *n*-alkan-1,15-diols and the
445 corresponding C₃₀ keto-ols are also found in concentrations ranging from 7.30 to
446 35.81 $\mu\text{g g OC}^{-1}$, with an average of 20.3 $\mu\text{g g OC}^{-1}$ (Table 3).

447 ΣMar range between 18.2 to 72.6 $\mu\text{g g OC}^{-1}$, 43.6 $\mu\text{g g OC}^{-1}$ on average (Fig. 4d and
448 Table 3), displaying a generally increasing eastward trend with maximum
449 concentrations (>55 $\mu\text{g g OC}^{-1}$) recorded in the deep northwestern Levantine Sea
450 (stations Red2.1, Her01, Ier01 and Red7). Elevated ΣMar values are also recorded
451 at stations Red3 in the upper slope of the western Cretan Straits, but also stations
452 H04 and H05 in the deep Ionian Sea. The lowest values (<40 $\mu\text{g g OC}^{-1}$) are
453 obtained in the southern Aegean Sea (stations Red8, Red9), the northern Ionian Sea
454 (station H12) and the western Cretan Straits (station H01).

455

456 **4.5 Multivariate analysis of geochemical parameters**

457 Three main principal components (PCs) are identified from PCA, accounting for
458 64.3% of the variation within the data set (23.8%, 22.8% and 17.7% for PC1, PC2
459 and PC3, respectively). PC1 is characterised by positive loadings for water depth,
460 ΣTerNA , $\Sigma\text{TerN-OH}$, ΣMar , UCM and negative loadings for CPI_{NA} and $\text{CPI}_{\text{N-OH}}$. The
461 highest positive loadings on PC2 are associated to %CaCO₃, %clay in the bulk
462 sediment and TN/OC values, while negative loadings are associated to %lithogenics.
463 Finally, the geochemical parameters with high positive loadings on PC3 are %OC,
464 %TN, and %clay of the lithogenic fraction, while those with negative loadings are
465 $\delta^{13}\text{C}$ and sorting of bulk sediment (Fig. 5a).

466 Factor scores on each PC display significant variability amongst the studied stations,
467 both within the same area and from one area to another (Fig. 5b). High positive factor
468 scores on PC1 are observed both in stations to the west (Ionian Sea) and east
469 (western Cretan Straits and northwestern Levantine Sea). For PC2, an eastward
470 increasing contribution of positive factor score values seems to exist, with the highest
471 ones located in the southern Aegean Sea and the northwestern Levantine Sea. In
472 contrast, the prevalence on PC3 is recorded in stations of the Ionian Sea and in parts
473 of the northwestern Levantine Sea (Ierapetra Basin).

474 The contents of CaCO₃ show an increasing north-south and west-east gradient (Figs.
475 3b and 5). In the southern Aegean Sea, the northwestern Levantine Sea and the
476 western Cretan Straits' stations, CaCO₃ contents are positively correlated to %clay of
477 the bulk sediment (r=0.48, p<0.05) and to alkenone concentrations (r=0.62, p<0.05).
478 Lithogenic contents are higher in the north and west (Ionian Sea) while being
479 significantly positively correlated to OC and TN contents (r=0.65 and r=0.72, p<0.05,
480 respectively, excluding stations BF15, H07 and H12 of the Ionian Sea). Furthermore,
481 OC and TN contents of stations deeper than 2100 m show a significant positive
482 correlation to water depth (r=0.54 and r=0.70, respectively, p<0.05). However, this is
483 not highlighted by the PCA. A significant positive correlation is also observed for OC
484 and TN contents in the analysed samples (r=0.87, p<0.0001) (Fig. 6a).

485 Surface sediments of the Ionian Sea show a significant (p<0.05) positive correlation
486 of OC and TN contents to %clay (r=0.80 and r=0.73), and a negative correlation to
487 %silt (r=-0.75 and r=-0.65) and D₅₀ of the lithogenic fraction (r=-0.79 and r=-0.83).
488 δ¹³C values (excluding station Red3 of the western Cretan Straits) are significantly
489 (p<0.05) and positively correlated to CaCO₃ contents (r=0.53), %clay of the bulk
490 sediment (r=0.65) and molar TN/OC ratios (r=0.53), and negatively correlated to
491 %OC (r=-0.46), %silt (r=-0.66) and D₅₀ (r=-0.59) of the bulk sediment.

492 Terrestrial lipid biomarkers concentrations (ΣTerNA and ΣTerN-OH) display a
493 significant positive correlation amongst them (r=0.95, p<0.0001), but also to %clay
494 (both with r=-0.55, p<0.05) and D₅₀ (r=0.62 and r=0.58, respectively, p<0.01) of the
495 bulk lithogenic fraction. Moreover, ΣTerNA and ΣTerN-OH show a significant positive
496 correlation (p<0.05) to β-Sitosterol (₂₉Δ⁵) (r=0.71 and r=0.56, respectively, excluding
497 stations H07 and H12 of the Ionian Sea). ΣTerNA and ΣTerN-OH (not normalized to
498 OC contents) are also significantly correlated to OC (r=0.81 and r=0.76, respectively,
499 p<0.001), again excluding stations H07 and H12 of the Ionian Sea. ΣMar (not
500 normalized to OC contents) display a significant positive correlation with OC (r=0.7,
501 p<0.001), while a significant positive correlation (r>0.65, p<0.005 in all cases) is
502 evident amongst the concentration of cholesterol (₂₇Δ⁵) and marine algal markers
503 (₂₈Δ^{5,22E}, ₃₀Δ^{22E}, C₃₀ diols&keto-ols and alkenones; see Sect. 5.2.1).

504

505 **5 Discussion**

506 **5.1 Sources of sedimentary material in the deep Eastern Mediterranean Sea**

507 Clearly, the surface sediments of the deep EMS mostly consist of lithogenics and
508 carbonates, have low OC contents while opal is nearly absent (Table 2). The range
509 of lithogenics, carbonates and opal contents recorded in the investigated samples
510 are similar to those previously reported for the Eastern Mediterranean Sea
511 (Emelyanov and Shimkus, 1986; Bethoux, 1989; Cros, 1995; Kemp et al., 1999;
512 Rutten et al., 2000; Struck et al., 2001). OC contents reach values slightly above 1%
513 and are also comparable to those found in the Eastern Mediterranean Sea (0.56-
514 1.51%, Danovaro et al., 1993; 0.23-0.99%, Bianchi et al., 2003; 0.30-0.82%, Gogou
515 et al., 2000; 0.25-1.73%, Polymenakou et al., 2006), and relatively lower than those
516 found in the Western Mediterranean Sea (0.80-1.60%, Kaiser et al., 2014; 0.47-
517 1.53%, Masqué et al., 2003; 0.23-1.85%, Roussiez et al., 2006). Values found are
518 comparable to the typical hemipelagic sediments found in continental slopes
519 (Rullkötter, 2006) and slightly higher than those in deep basin areas (Seiter et al.,
520 2004).

521

522 **5.1.1 Lithogenics and carbonate**

523 The grain size of the lithogenic fraction found in the studied sediments is very similar
524 to that of Saharan dust particles, which mainly consist of clayey silts and silty clays
525 with diameters ranging from 0.5 to 60 μm ($D_{50} \sim 5 \mu\text{m}$) and two main modes at 3-4 μm
526 and 60 μm (Ratmeyer et al., 1999; Guerzoni and Molinaroli, 2005 and references
527 therein). This strongly suggests that the Sahara desert is the main source of
528 lithogenics to the deep EMS. This is further supported by observations pointing to
529 Saharan dust transported by southerlies blowing over the great North African desert
530 as the main lithogenic input to the EMS (Guerzoni et al., 1999; Weldeab et al., 2002).
531 The Saharan dust spreads rather uniformly across the EMS (Rutten et al., 2000;
532 Jickells et al., 2005). Furthermore, but to a lesser extent, volcanic ash deposition into
533 the EMS represents another external source of fine-grained particles (<5-50 μm)
534 (Kelepertsis et al., 2003). Mount Etna, located on the island of Sicily, generates

535 volcanic ash plumes that are transported by the wind reaching as far as Greece and
536 Libya (Olgun et al., 2013 and references therein).

537 Riverine inputs have a rather minor influence onto the open EMS sedimentation as
538 they are small and localized (Weldeab et al., 2002; Statham and Hart, 2005). The
539 relatively higher lithogenic contents found in most of the Ionian Sea stations (Fig. 3a
540 and Table 2) points to fluvial inputs reaching the area from the Adriatic Sea. The
541 main source of riverine inputs is the Po River, opening into the northernmost end of
542 the Adriatic Sea, although inputs from smaller rivers draining the Apennines could be
543 also relevant (Weldeab et al., 2002). In the Ionian Sea, river-sourced particles are
544 carried by both surface and deep currents flowing southwards along the Italian
545 Peninsula as part of the overall anticlockwise circulation in the Adriatic Sea (Orlic et
546 al., 1992). It should be noted that dense water formation takes place seasonally in
547 the Adriatic Sea, which triggers episodes of fast-flowing, sediment-loaded dense
548 near-bottom currents that cascade into the deeper Meso Adriatic depression before
549 passing through the Otranto Strait, subsequently spreading into the Ionian Sea where
550 their particle load settles to the bottom (e.g., Zocolotti and Salusti, 1987; Manca et
551 al., 2002; Canals et al., 2009).

552 The grain-size variability of the carbonate particles recorded in the studied sediment
553 samples is indicative of calcareous skeletons of primary producers. While the
554 abundance of particles $<8 \mu\text{m}$ is attributable to coccoliths, which is the most
555 abundant primary producer in the EMS (Emelyanov and Shimkus, 1986), coarser
556 carbonate particles mostly correspond to shells and fragments of calcareous
557 dinoflagellates and planktonic foraminifers, in agreement with Ziveri et al. (2000) and
558 Frenz et al. (2005). Although part of the carbonate fraction might also have a
559 terrestrial provenance as transported, for instance, with Saharan dust (Chester et al.,
560 1977; Correggiari et al., 1989; Rutten et al., 2000), this does not seem to be the case
561 with the investigated samples. Like other aeolian particles, aeolian carbonates are
562 typically better sorted than those formed *in situ*, as shown by a well-sorted unimodal
563 distribution due to gravitational settling during atmospheric transport (Skonieczny et
564 al., 2013). The predominance of very poorly sorted grain-size distributions within the
565 bulk sediment samples (Fig. 2a) and the highly variable CaCO_3 contents (Fig. 3b) in

566 the investigated samples, suggests that even within such a highly oligotrophic
567 environment biogenic carbonates are the main source of CaCO₃ in the deep EMS.

568

569 **5.1.2 Sources of sedimentary organic matter**

570 Bulk geochemical proxies such as elemental (TN/OC) and stable isotopic ratios of
571 OC ($\delta^{13}\text{C}$) have been widely used to assess the sources of OM in marine sediments
572 (Meyers, 1994; Goñi et al., 2003; Hu et al., 2006). Sedimentary molar TN/OC ratios
573 and $\delta^{13}\text{C}$ values determined in this study are consistent with values previously
574 reported for surface sediments of the deep EMS (Tesi et al., 2007b; Meyers and
575 Arnaboldi, 2008; Carlier et al., 2010; Goudeau et al., 2013).

576 Marine-derived OM is characterized by high TN contents yielding TN/OC ratio values
577 >0.12 , while vascular plants are N-depleted yielding TN/OC ratio values <0.08
578 (Redfield et al., 1963; Hedges and Oades, 1997). $\delta^{13}\text{C}$ values in marine algae from
579 low- to mid- latitude temperate seas vary from -18‰ to -22‰ (Goericke and Fry,
580 1994; Meyers, 1994; Harmelin-Vivien et al., 2008), whereas most terrestrial OM
581 inputs from C3 plants show depleted $\delta^{13}\text{C}$ values ranging from -25‰ to -28‰
582 (Hedges et al., 1997).

583 In order to constrain the origin of sedimentary OM and assess the spatial variability in
584 its marine-to-terrestrial blend molar TN/OC ratios were plotted against $\delta^{13}\text{C}$ values.
585 Plots show that the elemental and isotopic composition of sedimentary OM fall out of
586 the typical compositional ranges of the potential sources (Fig. 6b). Excluding station
587 Red3, located in the upper slope of western Cretan Straits, an overall positive
588 relationship for molar TN/OC ratios and $\delta^{13}\text{C}$ values ($r=0.53$, $p<0.05$) becomes
589 apparent (Fig. 6b), thus indicating that the composition of the OM in the studied
590 sediment samples could be explained as a mixture of terrigenous (low TN/OC and
591 $\delta^{13}\text{C}$) and marine (high TN/OC and $\delta^{13}\text{C}$) derived materials.

592 Additionally, the relative contribution of the marine vs. terrestrial sources of OC over
593 the study area has been evaluated by means of a simple $\delta^{13}\text{C}$ -based binary mixing
594 model (Table 2), where a marine $\delta^{13}\text{C}$ value of -20.4‰ and a terrestrial $\delta^{13}\text{C}$ value of
595 -27.0‰ (Tesi et al., 2007a) are assumed, considering that the contribution of C4

596 vascular plants ($\delta^{13}\text{C}$ from -12 to -15‰) can be considered negligible throughout the
597 study area (e.g., Collatz et al., 1998).

598 As evident in Table 2, sediments from the Ionian Sea are characterized by elevated
599 contributions of terrestrial OC (OC_{terr}), reaching up to 64.2%. In contrast, W Cretan
600 Straits, Cretan Sea and NW Levantine Sea stations show low OC_{terr} contributions
601 and marine OC (OC_{mar}) peaks of 87.7% (see also section 5.2). The elevated OC_{terr}
602 values recorded in the Ionian Sea suggest that terrigenous OM entering the Adriatic
603 Sea escapes towards the deep Ionian basins. Indeed, during energetic dense shelf
604 water cascading events, lateral flux prevails over the vertical flux in the southern
605 Adriatic Sea and the contribution of soil-derived OC increases up to ~60% (Turchetto
606 et al., 2007; Tesi et al., 2008). Despite the relatively high OC_{terr} found preserved in
607 the deep Ionian Sea, values are lower than those recorded in areas impacted by
608 extreme events such as storms that enhance the export of organic matter from the
609 shelf to the deep environment, for example in the western Mediterranean (up to 78%
610 of OC_{terr}) (Pedrosa-Pàmies et al., 2013) and the East China Sea (up to 90%)
611 (Selvaraj et al., 2015).

612 Lipid biomarkers have often been used as molecular proxies to identify specific
613 biological precursors of sedimentary OM (Meyers, 1997; Volkman, 2006). The
614 concentrations of the sedimentary lipid biomarkers determined in this study are fairly
615 comparable to those previously reported in areas devoid of significant fluvial
616 influence both in the Eastern and Western Mediterranean basins (Grimalt and
617 Albaigés, 1990; Gogou et al., 2000; Gogou and Stephanou, 2004; Kaiser et al.,
618 2014).

619 The patterns of long-chain *n*-alkanes and *n*-alkanols with elevated CPI_{NA} and $\text{CPI}_{\text{N-OH}}$
620 values (Sect 4.4; Table 3), respectively, indicate the presence of allochthonous
621 natural (terrigenous) inputs from epicuticular higher plant waxes (Eglinton and
622 Hamilton, 1967). Saharan dust is probably the main vector for the transport of small
623 charcoal-like fragments of burnt vegetation, leaf wax-derived lipids absorbed on
624 clays, and cuticular fragments into the open EMS, given the relatively minor direct
625 influence of riverine inputs (Gogou et al., 1996; Eglinton et al., 2002).

626 Lipid biomarkers preserved in the surface sediments of the study area also highlight
627 the contribution from autochthonous marine OM derived from *in situ* phytoplankton

628 production. More specifically, the abundance of brassicasterol ($_{28}\Delta^{5,22E}$) reveals the
629 presence of diatoms and prymnesiophytes, while dinosterol ($_{30}\Delta^{22E}$) is a major
630 compound in dinoflagellates (Volkman, 1986). The presence of long-chain alkenones
631 reflects the productivity from algal species of the *Prymnesiophyte* class, e.g.,
632 *Emiliania huxleyi* (Marlowe et al., 1984), which constitute the dominant primary
633 producers across the Mediterranean Sea (Ziveri et al., 2000; Triantaphyllou, 2004).
634 Regarding the long-chain C_{30} *n*-alkan-1,15-diols and the corresponding C_{30} keto-ols,
635 although their major sources remain unknown, microalgae of the genus
636 *Nannochloropsis* (class *Eustigmatophyceae*) are potential sources, while C_{30} keto-ols
637 might result from oxidation of the corresponding C_{30} diols (Volkman, 1986; Volkman
638 et al., 1999; Rampen et al., 2012).

639 In addition, while the abundance of cholesterol ($_{27}\Delta^5$) highlights the existence of
640 marine consumer organisms such as zooplankton and benthic animals (Grice et al.,
641 1998), β -sitosterol ($_{29}\Delta^5$) may derive from both terrigenous and marine sources
642 (Volkman, 1986). In the study area however, the positive correlation between
643 Σ TerNA (and Σ TerN-OH) and β -sitosterol argues for a dominant terrestrial origin for
644 this compound.

645 Aside from natural sources, the abundance of UCM indicates a contribution of
646 anthropogenic OM resulting in chronic oil pollution of the investigated sediments
647 (Parinos et al., 2013). UCM levels recorded in the deep EMS are comparable to
648 those reported for surface sediments in unpolluted coastal and/or open-sea areas
649 and are at least one order of magnitude lower than those reported for coastal areas
650 subjected to enhanced anthropogenic inputs (Gogou et al., 2000; Parinos et al.,
651 2013; Kaiser et al., 2014; Romero et al., 2015; and references therein). Two main
652 pathways have been identified for the introduction of petroleum hydrocarbons into the
653 deep EMS, which are direct discharges from merchant shipping and oil transportation
654 (UNEP, 2010) and atmospheric transport and deposition (Gogou et al., 1996; Castro-
655 Jiménez et al., 2012; Parinos et al., 2013).

656 **5.2 Regional variability and oceanographic control on the geochemical**
657 **composition of deep Eastern Mediterranean Sea surface sediments**

658 The PCA provides a robust overview of the variables and processes controlling the
659 geochemical composition of the investigated deep-sea surface sediments (Fig. 5).

660 The significant positive loadings of ΣTerNA , $\Sigma\text{TerN-OH}$, ΣMar , UCM and depth on
661 PC1 are indicative of a considerable contribution from both natural (marine and
662 terrestrial) and anthropogenic (degraded petroleum products) OM preserved in deep-
663 sea surface sediments of the EMS. Moreover, the negative PC1 loadings of CPI_{NA}
664 and $\text{CPI}_{\text{N-OH}}$ ratios vs. depth indicate that the terrestrial OM is relatively altered with
665 increasing water column depth. Although the negative PC1 loading of CPI_{NA} ratio
666 could be also indicative of an enhanced contribution from non degraded petroleum
667 inputs, the patterns of aliphatic hydrocarbons for the investigated sediment samples
668 indicate no important bias associated to non degraded petroleum products on CPI_{NA}
669 ratio values (Parinos et al., 2013). Overall, PC1 represents the degradation
670 processes and fate of the sedimentary OM in the study area.

671 The second PC separates samples with high carbonate contents, molar TN/OC ratios
672 and enhanced contribution of clay-sized particles from those with high lithogenic
673 contents. Therefore, samples with positive loadings on PC2 are enriched in fine
674 marine carbonate particles, while those with negative loadings are enriched in
675 lithogenic particles (see section 5.2.2).

676 Finally, PC3 separates samples with high contents of OC, TN and clays from those
677 with high values of $\delta^{13}\text{C}$. Consequently, positive loadings on PC3 are associated to
678 sediments with an enhanced contribution of OC-rich fine particles, thus pointing to
679 hydrodynamic processes that control grain size sorting and remobilization/deposition
680 of sedimentary material with different OC contents (see section 5.2.2).

681

682 **5.2.1 Processes modulating the biogeochemical signal of the sedimentary**
683 **organic matter**

684 The low OC and TN contents in the surface sediments of the study area reflect the
685 oligotrophic character of the EMS (e.g., Krom et al., 2003). In the studied sediments
686 some processes may have further pushed TN to OC ratios towards low values (Fig.

687 6a). These include the preferential degradation of N-rich proteinaceous components
688 of algal OM during early diagenesis (Meyers et al., 1996; Meyers, 1997; Hopmans et
689 al., 2004) and the enrichment of OC relative to TN due to the input of petroleum
690 residues (Frigos et al., 1998). Furthermore, a significant contribution of inorganic N,
691 presumably as NH_4^+ adsorbed on clays (Müller, 1977; Meyers, 1997), is inferred
692 from the positive intercept on the N axis at around 0.02% (Fig. 6a).

693 Although isotopic fractionation specifically associated with early diagenesis is
694 negligible and the isotopic composition of sedimentary OM is fairly conservative (e.g.,
695 Di Leonardo et al., 2009 and references therein), $\delta^{13}\text{C}$ values can be potentially
696 shifted by microbial rearrangements (Lehmann et al., 2002) and inputs of
697 anthropogenic OM. $\delta^{13}\text{C}$ values for crude oil and petroleum products are in the order
698 of -28.5‰ and -28.9‰, respectively (Rumolo et al., 2011 and references therein). In
699 the study area, the positive PC1 loadings of depth and UCM indicate an enhanced
700 contribution of degraded petroleum products with increasing water depth. This points
701 to an enrichment of the sediments in degraded petroleum hydrocarbons in the deep
702 Ionian Sea and western Cretan Straits' stations H03 and Red3.1 where such an
703 isotopic shift is observed (Figs. 3e and 7), in addition to maximum concentrations of
704 UCM along with relatively low molar TN/OC ratios (<0.11) (Table 2, Figs. 3d and 4a).

705 Lipid biomarkers provide further information on the natural sources of sedimentary
706 OM. The significant positive correlation of ΣTerNA and $\Sigma\text{TerN-OH}$ concentrations
707 (not normalized to OC) to OC contents suggests a close association of terrestrial OM
708 to OC, while the significant positive correlation of ΣTerNA and $\Sigma\text{TerN-OH}$ to %clay
709 suggests that the transport and accumulation of terrestrial OM is associated to fine
710 particles (see section 5.2.2). The relatively uniform spatial distribution of CPI_{NA} and
711 $\text{CPI}_{\text{N-OH}}$ ratio values (Fig. 8) together with the negative PC1 loadings of CPI_{NA} and
712 $\text{CPI}_{\text{N-OH}}$ ratios vs. depth (Fig. 5), are overall indicative of the reworking of the
713 terrestrial OM accumulated in deep EMS basins. Moreover, the elevated values of
714 the $[\text{NA}]/[\text{N-OH}]$ ratio in the study area (Fig.8; Table 3) are indicative of the enhanced
715 degradation of $\Sigma\text{TerN-OH}$ relatively to ΣTerNA . The above are rather consistent with
716 the long-range atmospheric transport, and long residence time in the water column
717 and into the sediments of the terrestrial OM, and the fact that ΣTerNA are more
718 resistant to degradation than their alcohol counterparts (Gogou and Stephanou,

719 2004). Moreover, the relatively elevated retention time of terrestrial OC in the inner
720 shelf of the Adriatic Sea before being conveyed to the Ionian Sea by dense shelf
721 water cascading events, allows for its significant microbial degradation or marine
722 dilution (Tesi et al., 2008).

723 While a significant positive correlation is observed for Σ Mar concentrations (not
724 normalized to OC contents) and OC, indicating that the latter exerts an important
725 control on the distribution of algal markers' concentrations in the study area, no
726 significant correlation is observed between Σ Mar and grain size. These correlations
727 together with the deviation trend observed for molar TN/OC ratios from the classical
728 Redfield ratio (16/106) with increasing water depth, which is more evident for the
729 deep Ionian Sea stations (Fig. 6a), probably reflect the preferential degradation
730 processes during the transport and deposition of marine labile sedimentary OM, that
731 probably also masks the association of marine OM to fine particles. The observations
732 above, jointly with the presence of cholesterol ($_{27}\Delta^5$) and its significant positive
733 correlation with the concentrations of marine algal markers, are altogether indicative
734 of the re-working of algal OM by zooplankton and benthic invertebrates (Volkman et
735 al., 1990; Gogou and Stephanou, 2004).

736

737 **5.2.2 Sediment transport and deposition processes**

738 The second and third PCs of the PCA highlight the main processes that affect
739 sediment dispersal and deposition in the study area. These relate to pelagic settling
740 of marine skeletons from surface waters (corresponding to PC2), and hydrodynamic
741 sorting of organic-rich fine sediment by bottom currents (corresponding to PC3).

742 Particulate matter exported from the upper layers of the water column in the EMS is
743 primarily composed of biogenic particles and atmospheric dust, which while settling
744 to the seabed are able to transfer OC, other nutrient elements, and OC-associated
745 organic pollutants (e.g., Stavrakakis et al., 2000, 2013; Theodosi et al., 2013). In the
746 deep EMS, the distribution of pelagic carbonates (second PC) seems to be mainly
747 influenced by planktonic contributions. In the study area, the phytoplankton biomass
748 and primary production are relatively higher in regions of cyclonic water mass
749 circulation. The Rhodes cold-core gyre, situated in the southeast of the Rhodes

750 Island (NW Levantine Sea), is the most prominent dynamic feature in the EMS and is
751 the main source area of the LIW. In this cyclonic gyre, which is enhanced during
752 winter period, dense water masses from deeper layers tend to upwell at its centre,
753 feeding the upper layers with nutrient-rich waters (Salihoğlu et al., 1990). Therefore,
754 this gyre plays an important role in the productivity of the Levantine Sea.

755 The third PC separated samples with high OC, TN and clay contents, which is
756 indicative of a close OM-mineral association. This is in agreement with the high OC
757 contents found in the fine-grained sediment samples from the deeper stations
758 representing an essentially quiet environment (Figs. 2, 3 and 7). This is in contrast to
759 the lower OC contents observed in coarser samples ($D_{50} > 14 \mu\text{m}$) from shallower
760 depths where currents up to 20 cm s^{-1} occur commonly (Kontoyiannis et al., 2005;
761 Ursella et al., 2014). Fine-grained particles have high capacity for OM adsorption due
762 to their large specific surface area, and thus enhanced OM contents relatively to
763 coarse-grained particles (Mayer, 1994; Hedges and Keil, 1995). Physical processes
764 such as hydrodynamic sorting remobilize and transport sedimentary material with
765 different OC contents, with the OC-rich finest ones easily reaching the deep EMS. A
766 similar situation has been reported in active sedimentary environments such as the
767 submarine canyons in the Western Mediterranean Sea (Pedrosa-Pàmies et al.,
768 2013), the northwestern Gulf of Mexico (Goñi et al., 1998) and the Peru Margin
769 (Bergamaschi et al., 1997). However, none of these studies reported such OM-
770 mineral associations at depths beyond 4000m. This indicates that this organic-
771 mineral interaction is maintained from the shallow to high depths, which constitute
772 the final sedimentary sink. In short, the deep EMS behaves as a depocenter for OM-
773 rich fine particles.

774 Moreover, in the EMS these bulk sediments show a poorer sorting than the lithogenic
775 fraction (Fig. 2). This could be related to the presence of coarse biogenic carbonate
776 particles in bulk samples or the effective hydrodynamic sorting linked to the prevailing
777 depositional conditions in such deep low-energy environments (Friedman, 1969).

778 The poor sorting and positive skewness found in grain-size types I, II, IV and V of the
779 bulk sediment samples (Fig. 2a) in the southern Aegean Sea and the northwestern
780 Levantine Sea, is explained by the prevalence of pelagic biogenic sedimentation, as
781 shown by the high positive score values observed on PC2 (Fig. 5b). Accordingly,

782 high percentages of CaCO_3 have been measured in stations of the southern Aegean
783 Sea, the northwestern Levantine Sea and western Cretan Straits, which correlate to
784 %clay fraction of the bulk sediment samples and the concentrations of alkenones
785 (Table 3). This links to the formation of clay-carbonate concretions that have been
786 reported in particularly large amounts in the southern Aegean Sea (Emelyanov and
787 Shimkus, 1986). Vertical mixing and upward transport of nutrients in the eddies and
788 gyres, such as the Rhodes gyre, may trigger primary production and subsequently
789 the sinking and dominance of pelagic biogenic particles over particles from other
790 sources in the northwestern Levantine Sea (Siokou-Frangou et al., 1999). The
791 %OC_{mar} and the ΣMar distribution are indicative in that respect as they show a
792 general eastward increasing trend with peak concentrations in deep basins of the
793 northwestern Levantine Sea.

794 Surface sediments in the Ierapetra Basin (stations Red15, Red1.1 and Ier01) also
795 show positive scores on PC3 (Fig. 5b), which point to an influence of hydrodynamic
796 sorting processes. The relatively high OC content in these stations (Fig. 7), along
797 with the elevated values of the associated natural and anthropogenic lipid
798 concentrations (Table 3), suggests that the Hellenic Trench is a sink of OC
799 associated to fine particles transferred by the active outflows of the Cretan Straits,
800 besides the pelagic sedimentation related to the well-known semi-permanent
801 Ierapetra anticyclone (Larnicol et al., 2002; Taupier-Letage, 2008).

802 Sediments with grain size types I-III of the bulk sediment samples (Fig. 2a) in the
803 Ionian Sea show lower CaCO_3 contents due to the dilution by lithogenic components,
804 with station H02 being the only exception. High positive score values on PC3 (Fig.
805 5b), and the significant positive correlation for OC and TN contents to %clay of the
806 lithogenic fraction, further suggest a significant influence of hydrodynamic sorting
807 processes, which largely determine a differential distribution of OM in surface
808 sediments according to grain size. In this area, the Otranto Strait may act as a
809 preferential conduit by funnelling fine OC-rich particles from the Adriatic Sea towards
810 the deep basins of the adjacent Ionian Sea, which may eventually reach the
811 Levantine Sea (Bensi et al., 2013). The enhanced contributions of OC_{terr} (Table 2)
812 and terrestrial biomarkers concentrations (Figs. 4b-c and Table 3) of the Ionian
813 samples off the southern mouth of the Adriatic Sea, probably also reflect the

814 preferential degradation of labile marine OM in deep Ionian Sea basins due to slower
815 sedimentation rates and longer residence time of OM. Low OC content (Fig. 3c), poor
816 sorting, very negatively skewed, high %sand of grain size type VI (Fig. 2a) at the
817 shallower station H12 just south of Otranto Strait supports winnowing of fine OC-rich
818 particles due to episodic events of high current speed exiting the Adriatic Sea
819 (Bignami et al., 1991; Gacic et al., 1996; Poulos et al., 1999).

820 Finally, station Red3 from the upper slope of western Cretan Straits representing
821 grain size type VII of the bulk sediment samples (Fig. 2a) shows the highest contents
822 of sand (47.7%), which is poorly sorted. This is in agreement with the occurrence of
823 the topographically restricted deep outflow of the western Cretan Straits. These
824 straits are characterized by maximum outflow speeds during winter and minimum
825 speeds during fall (Kontoyiannis et al., 2005). The turbulent, fluctuating outflow
826 current should normally trigger sediment resuspension and induce selective
827 transport, thus leaving coarse OC-poor particles in the upper slope of the western
828 Cretan Straits (negative factor scores of PC2 and PC3) and carrying fine OC-rich
829 particles to the lower slope. A similar pattern has been also observed in other
830 submarine canyon settings of the Mediterranean Sea, such as the Cap de Creus
831 Canyon (Sanchez-Vidal et al., 2008) and the Blanes Canyon (Pedrosa-Pàmies et al.,
832 2013). The top $\delta^{13}\text{C}$ values found in the upper slope (Fig. 7 and Tables 2-3) indicates
833 high contribution of marine OC, which however is not supported by the lipid
834 biomarkers results. Winnowing of fine particles loaded with terrestrial OC, thus
835 shifting the isotopic signal of the remaining coarse particles towards high and more
836 marine values seems to be the most plausible explanation.

837

838 **6 Conclusions**

839 Surface sediments collected from deep basins of the oligotrophic EMS were
840 investigated using a multi-proxy approach that involved elemental composition, grain
841 size, stable isotopes and selected lipid biomarkers' analyses resulting in a robust
842 database to determine sediment sources, the degradation and preservation state of
843 OM, and processes that affect sediment dispersal and deposition. The PCA analysis
844 helped to identify the main controlling factors of the observed geochemical variability
845 in the investigated sediments. Such factors are sediment sources in terms of

846 allochthonous vs. autochthonous, a highly variable physiography, the thermohaline
847 structure, and the regional and local circulation, leading to hydrodynamic sorting and
848 regulating particle settling/deposition and OM preservation state.

849 Surface sediments of the investigated part of the EMS mostly consist of airborne
850 lithogenic particles and biogenic carbonate particles, the latter deriving from primary
851 production into surface waters. Sedimentary OM appears in rather low contents (0.15
852 – 1.15% OC), with bulk and molecular organic tracers reflecting a mixed contribution
853 from both natural (autochthonous and allochthonous) and anthropogenic sources.
854 Samples from locations in the Ionian Sea and the western Cretan Straits that are
855 under the direct influence of the Adriatic dense waters outflow through the Otranto
856 Strait and of currents exiting the southern Aegean Sea, respectively, are appreciably
857 sorted. Current regime impacted not only grain size but also OC loadings within each
858 subregion of the study area, with winnowing of fine OC-rich particles to the deepest
859 EMS. In contrast, coarse OC-poor particles tend to occur in upper slope settings.
860 While OC associated to fine particles was relatively non-degraded terrestrial OM,
861 marine OM was found to be mostly degraded and reworked during transport
862 processes and before reaching the deep seafloor.

863 The spatial variability in the yields of sedimentary OC and lipid biomarkers presented
864 in this study highlights the heterogeneous nature of the particle load exported to the
865 deep basins of the Eastern Mediterranean Sea. Such variability must be taken into
866 account during the development of quantitative carbon budgets for this area.

867

868 **Acknowledgements**

869 This research has been supported by the EU-funded project PERSEUS (GA
870 287600), the EU-Greek co-funded project KRIPIS (MIS 451724; NSRF) and
871 REDECO (CTM2008-04973-E/MAR), BIOFUN (CTM2007-28739-E) and MEDECOS
872 (Σ AE 013/8 -2010 Σ E01380001) projects. Researchers from GRC Geociències
873 Marines benefited from a *Grups de Recerca Consolidats* grant 2014 SGR 1068 by
874 the *Generalitat de Catalunya* autonomous government. We sincerely thank chief
875 scientist K.C. Emeis (*R/V Meteor*) and the officers and crews of *R/V Meteor*, *R/V*

876 *Aegaeo* and *R/V Sarmiento de Gamboa* for their precious help during the cruises.
877 Elemental and isotopic analyses have been performed at the Scientific-Technical
878 Services of the University of Barcelona. R.P.-P. is supported by a predoctoral FPU
879 grant and A.S.-V. by a Ramon y Cajal contract. Dr. Juergen Mobius is acknowledged
880 for his constructive comments on an earlier version of the manuscript. We would like
881 to thank the Editor and Dr. T. Tesi and three anonymous referees for their
882 constructive comments that helped us significantly improve the quality of the
883 manuscript during the revision process.

884

885 **References**

- 886 Amblàs, D., Canals, M., Lastras, G., Berné, S. and Loubrieu, B.: Imaging the Seascapes of the
887 Mediterranean, *Oceanography*, 17(4), 144–155, doi:10.5670/oceanog.2004.11, 2004.
- 888 Bensi, M., Cardin, V., Rubino, A., Notarstefano, G. and Poulain, P. M.: Effects of winter
889 convection on the deep layer of the Southern Adriatic Sea in 2012, *J. Geophys. Res. Ocean.*,
890 118(11), 6064–6075, doi:10.1002/2013JC009432, 2013.
- 891 Bergamaschi, B. a., Tsamakis, E., Keil, R. G., Eglinton, T. I., Montluçon, D. B. and Hedges,
892 J. I.: The effect of grain size and surface area on organic matter, lignin and carbohydrate
893 concentration, and molecular compositions in Peru Margin sediments, *Geochim. Cosmochim.*
894 *Acta*, 61(6), 1247–1260, doi:10.1016/S0016-7037(96)00394-8, 1997.
- 895 Bethoux, J. P.: Budgets of the Mediterranean Sea. Their dependence on the local climate and
896 on the characteristics of the Atlantic waters, *Oceanol. Acta*, 2, 157–163, 1979.
- 897 Bethoux, J. P.: Oxygen consumption, new production, vertical advection and environmental
898 evolution in the Mediterranean Sea, *Deep Sea Res. Part A. Oceanogr. Res. Pap.*, 36(5), 769–
899 781, doi:10.1016/0198-0149(89)90150-7, 1989.
- 900 Bianchi, A., Tholosan, O., Garcin, J., Polychronaki, T., Tselepides, A., Buscail, R. and
901 Duineveld, G.: Microbial activities at the benthic boundary layer in the Aegean Sea, *Prog.*
902 *Oceanogr.*, 57(2), 219–236, doi:10.1016/S0079-6611(03)00034-X, 2003.
- 903 Blott, S. J. and Pye, K.: GRADISTAT: A grain size distribution and statistics package for the
904 analysis of unconsolidated sediments, *Earth Surf. Process. Landforms*, 26(11), 1237–1248,
905 doi:10.1002/esp.261, 2001.
- 906 Bosc, E., Bricaud, A. and Antoine, D.: Seasonal and interannual variability in algal biomass
907 and primary production in the Mediterranean Sea, as derived from 4 years of SeaWiFS
908 observations, *Global Biogeochem. Cycles*, 18(1), GB1005, doi:10.1029/2003GB002034,
909 2004.

- 910 Bouloubassi, I., Lipiatou, E., Saliot, A., Tolosa, I., Bayona, J. M. and Albaigés, J.: Carbon
911 sources and cycle in the western Mediterranean-the use of molecular markers to determine the
912 origin of organic matter, *Deep Sea Res. Part II Top. Stud. Oceanogr.*, 44(3-4), 781–799,
913 doi:10.1016/S0967-0645(96)00094-X, 1997.
- 914 Burdige, D. J.: Preservation of organic matter in marine sediments: controls, mechanisms, and
915 an imbalance in sediment organic carbon budgets?, *Chem. Rev.*, 107(2), 467–85,
916 doi:10.1021/cr050347q, 2007.
- 917 Canals, M., Danovaro, R., Heussner, S., Lykousis, V., Puig, P., Trincardi, F., Calafat, A.,
918 Durrieu de Madron, X. and Palanques, A.: Cascades in Mediterranean Submarine Grand
919 Canyons, *Oceanography*, 22(1), 26–43, doi:10.5670/oceanog.2009.03, 2009.
- 920 Carlier, A., Ritt, B., Rodrigues, C. F., Sarrazin, J., Olu, K., Grall, J. and Clavier, J.:
921 Heterogeneous energetic pathways and carbon sources on deep eastern Mediterranean cold
922 seep communities, *Mar. Biol.*, 157(11), 2545–2565, doi:10.1007/s00227-010-1518-1, 2010.
- 923 Castro-Jiménez, J., Berrojalbiz, N., Wollgast, J. and Dachs, J.: Polycyclic aromatic
924 hydrocarbons (PAHs) in the Mediterranean Sea: atmospheric occurrence, deposition and
925 decoupling with settling fluxes in the water column., *Environ. Pollut.*, 166, 40–7,
926 doi:10.1016/j.envpol.2012.03.003, 2012.
- 927 Chester, R., Baxter, G. G., Behairy, A. K. A., Connor, K., Cross, D., Elderfield, H. and
928 Padgham, R. C.: Soil-sized eolian dusts from the lower troposphere of the eastern
929 Mediterranean Sea, *Mar. Geol.*, 24(3), 201–217, doi:10.1016/0025-3227(77)90028-7, 1977.
- 930 Collatz, G. J., Berry, J. a. and Clark, J. S.: Effects of climate and atmospheric CO₂ partial
931 pressure on the global distribution of C₄ grasses: present, past, and future, *Oecologia*, 114(4),
932 441–454, doi:10.1007/s004420050468, 1998.
- 933 Collister, J. W., Rieley, G., Stern, B., Eglinton, G. and Fry, B.: Compound-specific $\delta^{13}\text{C}$
934 analyses of leaf lipids from plants with differing carbon dioxide metabolisms, *Org. Geochem.*,
935 21(6-7), 619–627, doi:10.1016/0146-6380(94)90008-6, 1994.
- 936 Correggiari, A., Guerzoni, S., Lenaz, R., Quarantotto, G. and Rampazzo, G.: Dust deposition
937 in the central Mediterranean (Tyrrhenian and Adriatic Seas): Relationships with marine
938 sediments and riverine input, *Terra Nov.*, 1(6), 549–558, doi:10.1111/j.1365-
939 3121.1989.tb00431.x, 1989.
- 940 Cros, L.: Calcareous nannoplankton in surficial sediments of the Catalano-Balearic Sea
941 (northeastern Mediterranean), in *5Th INA Conference in Salamanca Proceedings*, pp. 47–59.,
942 1995.
- 943 Danovaro, R., Fabiano, M. and Della Croce, N.: Labile organic matter and microbial
944 biomasses in deep-sea sediments (Eastern Mediterranean Sea), *Deep Sea Res. Part I*
945 *Oceanogr. Res. Pap.*, 40(5), 953–965, doi:10.1016/0967-0637(93)90083-F, 1993.
- 946 Danovaro, R., Company, J. B., Corinaldesi, C., D’Onghia, G., Galil, B., Gambi, C., Gooday,
947 A. J., Lampadariou, N., Luna, G. M., Morigi, C., Olu, K., Polymenakou, P. N., Ramirez-

- 948 Llodra, E., Sabbatini, A., Sardà, F., Sibuet, M. and Tselepides, A.: Deep-sea biodiversity in
949 the Mediterranean Sea: the known, the unknown, and the unknowable., *PLoS One*, 5(8),
950 e11832, doi:10.1371/journal.pone.0011832, 2010.
- 951 Durrieu de Madron, X., Abassi, A., Heussner, S., Monaco, A., Aloisi, J. C., Radakovitch, O.,
952 Giresse, P., Buscail, R. and Kerherve, P.: Particulate matter and organic carbon budgets for
953 the Gulf of Lions (NW Mediterranean), *Oceanol. Acta*, 23(6), 717–730, doi:10.1016/S0399-
954 1784(00)00119-5, 2000.
- 955 Eglinton, G. and Hamilton, R. J.: Leaf Epicuticular Waxes, *Science* (80-.), 156(3780), 1322–
956 1335, doi:10.1126/science.156.3780.1322, 1967.
- 957 Eglinton, T. I., Eglinton, G., Dupont, L., Sholkovitz, E. R., Montluçon, D. and Reddy, C. M.:
958 Composition, age, and provenance of organic matter in NW African dust over the Atlantic
959 Ocean, *Geochemistry, Geophys. Geosystems*, 3(8), 1–27, 2002.
- 960 Ehrmann, W., Schmiedl, G., Hamann, Y., Kuhnt, T., Hemleben, C. and Siebel, W.: Clay
961 minerals in late glacial and Holocene sediments of the northern and southern Aegean Sea,
962 *Palaeogeogr. Palaeoclimatol. Palaeoecol.*, 249(1-2), 36–57, doi:10.1016/j.palaeo.2007.01.004,
963 2007.
- 964 Emelyanov, E. M. and Shimkus, K. M.: *Geochemistry and Sedimentology of the*
965 *Mediterranean Sea*, D. Reidel Publishing Company, Dordrecht, Holland., 1986.
- 966 Folk, R. L. and Ward, W. C.: Brazos River bar: A study in the significance of grain size
967 parameters, *J. Sediment. Res.*, 27(1), 3–26, doi:10.1306/74D70646-2B21-11D7-
968 8648000102C1865D, 1957.
- 969 Frenz, M., Baumann, K. H., Boeckel, B., Hoppner, R. and Henrich, R.: Quantification of
970 foraminifer and coccolith carbonate in South Atlantic surface sediments by means of
971 carbonate grain-size distributions, *J. Sediment. Res.*, 75(3), 464–475,
972 doi:10.2110/jsr.2005.036, 2005.
- 973 Friedman, G. M.: Trace elements as possible environmental indicators in carbonate
974 sediments, *Depos. Environ. Carbonate Rocks*, 193–198, 1969.
- 975 Friligos, N., Moriki, A., Sklivagou, E., Krasakopoulou, E. and Hatzianestis, I.: Geochemical
976 characteristics of the surficial sediments of the Aegean Sea, in 3rd MTP-MATER Workshop,
977 vol. 35, pp. 28–209, Rhodos., 1998.
- 978 Garcia-Orellana, J., Pates, J. M., Masqué, P., Bruach, J. M. and Sanchez-Cabeza, J. A.:
979 Distribution of artificial radionuclides in deep sediments of the Mediterranean Sea., *Sci. Total*
980 *Environ.*, 407(2), 887–98, doi:10.1016/j.scitotenv.2008.09.018, 2009.
- 981 Goericke, R. and Fry, B.: Variations of marine plankton $\delta^{13}\text{C}$ with latitude, temperature, and
982 dissolved CO_2 in the world ocean, *Global Biogeochem. Cycles*, 8(1), 85–90,
983 doi:10.1029/93GB03272, 1994.

- 984 Gogou, A. and Stephanou, E. G.: Marine organic geochemistry of the Eastern Mediterranean,
985 *Mar. Chem.*, 85(1-2), 1–25, doi:10.1016/j.marchem.2003.08.005, 2004.
- 986 Gogou, A., Stratigakis, N., Kanakidou, M. and Stephanou, E. G.: Organic aerosols in Eastern
987 Mediterranean: components source reconciliation by using molecular markers and
988 atmospheric back trajectories, *Org. Geochem.*, 25(1-2), 79–96, doi:10.1016/S0146-
989 6380(96)00105-2, 1996.
- 990 Gogou, A., Apostolaki, M. and Stephanou, E. G.: Determination of organic molecular
991 markers in marine aerosols and sediments: one-step flash chromatography compound class
992 fractionation and capillary gas chromatographic analysis, *J. Chromatogr. A*, 799(1-2), 215–
993 231, doi:10.1016/S0021-9673(97)01106-0, 1998.
- 994 Gogou, A., Bouloubassi, I. and Stephanou, E. G.: Marine organic geochemistry of the Eastern
995 Mediterranean: 1. Aliphatic and polyaromatic hydrocarbons in Cretan Sea surficial sediments,
996 *Mar. Chem.*, 68(4), 265–282, doi:10.1016/S0304-4203(99)00082-1, 2000.
- 997 Gogou, A., Bouloubassi, I., Lykousis, V., Arnaboldi, M., Gaitani, P. and Meyers, P. A.:
998 Organic geochemical evidence of Late Glacial–Holocene climate instability in the North
999 Aegean Sea, *Palaeogeogr. Palaeoclimatol. Palaeoecol.*, 256(1-2), 1–20,
1000 doi:10.1016/j.palaeo.2007.08.002, 2007.
- 1001 Gogou, A., Sanchez-Vidal, A., Durrieu de Madron, X., Stavrakakis, S., Calafat, A., Stabholz,
1002 M., Psarra, S., Canals, M., Heussner, S., Stavrakaki, I. and Papathanassiou, E.: Carbon flux to
1003 the deep in three open sites of the Southern European Seas (SES), *J. Mar. Syst.*, 129, 224–
1004 233, doi:10.1016/j.jmarsys.2013.05.013, 2014a.
- 1005 Gogou, A., Sanchez-Vidal, A., Durrieu de Madron, X., Stavrakakis, S., Calafat, A., Stabholz,
1006 M., Psarra, S., Canals, M., Heussner, S., Stavrakaki, I. and Papathanassiou, E.: Carbon flux to
1007 the deep in three open sites of the Southern European Seas (SES), *J. Mar. Syst.*, 129, 224–
1008 233, doi:10.1016/j.jmarsys.2013.05.013, 2014b.
- 1009 Goñi, M. A., Ruttenger, K. C. and Eglinton, T. I.: A reassessment of the sources and
1010 importance of land-derived organic matter in surface sediments from the Gulf of Mexico,
1011 *Geochim. Cosmochim. Acta*, 62(18), 3055–3075, doi:10.1016/S0016-7037(98)00217-8, 1998.
- 1012 Goñi, M. A., Teixeira, M. J. and Perkey, D. W.: Sources and distribution of organic matter in
1013 a river-dominated estuary (Winyah Bay, SC, USA), *Estuar. Coast. Shelf Sci.*, 57(5-6), 1023–
1014 1048, doi:10.1016/S0272-7714(03)00008-8, 2003.
- 1015 Goñi, M. A., Monacci, N., Gisewhite, R., Ogston, A., Crockett, J. and Nittrouer, C.:
1016 Distribution and sources of particulate organic matter in the water column and sediments of
1017 the Fly River Delta, Gulf of Papua (Papua New Guinea), *Estuar. Coast. Shelf Sci.*, 69, 225–
1018 245, doi:10.1016/j.ecss.2006.04.012, 2006.
- 1019 Goudeau, M.-L. S., Grauel, A.-L., Bernasconi, S. M. and de Lange, G. J.: Provenance of
1020 surface sediments along the southeastern Adriatic coast off Italy: An overview, *Estuar. Coast.
1021 Shelf Sci.*, 134, 45–56, doi:10.1016/j.ecss.2013.09.009, 2013.

- 1022 Gough, M. A. and Rowland, S. J.: Characterization of unresolved complex mixtures of
1023 hydrocarbons in petroleum, *Nature*, 344(6267), 648–650, doi:10.1038/344648a0, 1990.
- 1024 Grice, K., Klein Breteler, W., Schouten, S., Grossi, V., Leeuw, J. W. and Damsté, J. S. S.:
1025 Effects of zooplankton herbivory on biomarker proxy records, *Paleoceanography*, 13(6), 686–
1026 693, doi:10.1029/98PA01871, 1998.
- 1027 Grimalt, J. O. and Albaigés, J.: Characterization of the depositional environments of the Ebro
1028 Delta (western Mediterranean) by the study of sedimentary lipid markers, *Mar. Geol.*, 95(3-
1029 4), 207–224, doi:10.1016/0025-3227(90)90117-3, 1990.
- 1030 Guerzoni, S. and Molinaroli, E.: Input of Various Chemicals Transported by Saharan Dust
1031 and Depositing at the Sea Surface in the Mediterranean Sea, *Environmental Chem.*, 5, 237–
1032 268, doi:10.1007/b107149, 2005.
- 1033 Guerzoni, S., Chester, R., Dulac, F., Herut, B., Lojze-Pilot, M.-D., Measures, C., Migon, C.,
1034 Molinaroli, E., Moulin, C., Rossini, P., Saydam, C., Soudine, A. and Ziveri, P.: The role of
1035 atmospheric deposition in the biogeochemistry of the Mediterranean Sea, *Prog. Oceanogr.*,
1036 44(1-3), 147–190, doi:10.1016/S0079-6611(99)00024-5, 1999.
- 1037 Hamann, Y., Ehrmann, W., Schmiedl, G., Krüger, S., Stuut, J.-B. and Kuhnt, T.:
1038 Sedimentation processes in the Eastern Mediterranean Sea during the Late Glacial and
1039 Holocene revealed by end-member modelling of the terrigenous fraction in marine sediments,
1040 *Mar. Geol.*, 248(1-2), 97–114, doi:10.1016/j.margeo.2007.10.009, 2008.
- 1041 Harmelin-Vivien, M., Loizeau, V., Mellon, C. and Beker, B.: Comparison of C and N stable
1042 isotope ratios between surface particulate organic matter and microphytoplankton in the Gulf
1043 of Lions (NW Mediterranean), *Cont. Shelf Res.*, 28(15), 1911–1919,
1044 doi:10.1016/j.csr.2008.03.002, 2008.
- 1045 Hedges, J. I. and Keil, R. G.: Sedimentary organic matter preservation: an assessment and
1046 speculative synthesis, *Mar. Chem.*, 49(2-3), 81–115, doi:10.1016/0304-4203(95)00008-F,
1047 1995.
- 1048 Hedges, J. I. and Oades, J. M.: Comparative organic geochemistries of soils and marine
1049 sediments, *Org. Geochem.*, 27(7-8), 319–361, doi:10.1016/S0146-6380(97)00056-9, 1997.
- 1050 Hedges, J. I., Keil, R. G. and Benner, R.: What happens to terrestrial organic matter in the
1051 ocean?, *Org. Geochem.*, 27(5-6), 195–212, doi:10.1016/S0146-6380(97)00066-1, 1997.
- 1052 Heussner, S., Calafat, A. and Palanques, A.: Quantitative and qualitative features of particle
1053 fluxes in the North-Balearic Basin, EUROMARGE-NB Final Report, Ed. by Canals, M.,
1054 Casamor, JL, Cacho, I., Calafat, AM, Monaco, A., MAST II Program. EC, 2, 41–66, 1996.
- 1055 Hopmans, E. C., Weijers, J. W. ., Schefuß, E., Herfort, L., Sinninghe Damsté, J. S. and
1056 Schouten, S.: A novel proxy for terrestrial organic matter in sediments based on branched and
1057 isoprenoid tetraether lipids, *Earth Planet. Sci. Lett.*, 224(1-2), 107–116,
1058 doi:10.1016/j.epsl.2004.05.012, 2004.

- 1059 Hu, J., Peng, P., Jia, G., Mai, B. and Zhang, G.: Distribution and sources of organic carbon,
1060 nitrogen and their isotopes in sediments of the subtropical Pearl River estuary and adjacent
1061 shelf, Southern China, *Mar. Chem.*, 98(2-4), 274–285, doi:10.1016/j.marchem.2005.03.008,
1062 2006.
- 1063 IOC, IHO and BODC: Centenary edition of the GEBCO digital atlas, published on CD-ROM
1064 on behalf of the Intergovernmental Oceanographic Commission and the International
1065 Hydrographic Organization as part of the General Bathymetric Chart of the Oceans,
1066 Liverpool, UK., 2003.
- 1067 Jickells, T. D.: Atmospheric inputs of metals and nutrients to the oceans: their magnitude and
1068 effects, *Mar. Chem.*, 48(3-4), 199–214, doi:10.1016/0304-4203(95)92784-P, 1995.
- 1069 Jickells, T. D., An, Z. S., Andersen, K. K., Baker, A. R., Bergametti, G., Brooks, N., Cao, J.
1070 J., Boyd, P. W., Duce, R. A., Hunter, K. A., Kawahata, H., Kubilay, N., laRoche, J., Liss, P.
1071 S., Mahowald, N., Prospero, J. M., Ridgwell, A. J., Tegen, I. and Torres, R.: Global iron
1072 connections between desert dust, ocean biogeochemistry, and climate., *Science*, 308(5718),
1073 67–71, doi:10.1126/science.1105959, 2005.
- 1074 Kaiser, J., Ruggieri, N., Hefter, J., Siegel, H., Mollenhauer, G., Arz, H. W. and Lamy, F.:
1075 Lipid biomarkers in surface sediments from the gulf of genoa, Ligurian sea (NW
1076 Mediterranean sea) and their potential for the reconstruction of palaeo-environments, *Deep
1077 Sea Res. Part I Oceanogr. Res. Pap.*, 89, 68–83, doi:10.1016/j.dsr.2014.04.009, 2014.
- 1078 Kelepertsis, A. E., Alexakis, D. E., Nastos, P. T. and Kanellopoulou, E. A.: The presence of
1079 volcanic ash in the western Greece and its association with the eruption of the Etna volcano,
1080 Italy. Consequences on the Environment., in 8th International Conference on Environmental
1081 Science and Technology, pp. 408–415, Lemnos Island, Greece., 2003.
- 1082 Kemp, A. E. S., Pearce, R. B., Koizumi, I., Pike, J. and Rance, S. J.: The role of mat-forming
1083 diatoms in the formation of Mediterranean sapropels, *Nature*, 398(6722), 57–61,
1084 doi:10.1038/18001, 1999.
- 1085 Kontoyiannis, H., Balopoulos, E., Gotsis-Skretas, O., Pavlidou, A., Assimakopoulou, G. and
1086 Papageorgiou, E.: The hydrology and biochemistry of the Cretan Straits (Antikithira and
1087 Kassos Straits) revisited in the period June 1997–May 1998, *J. Mar. Syst.*, 53(1-4), 37–57,
1088 doi:10.1016/j.jmarsys.2004.06.007, 2005.
- 1089 Krom, M. D., Groom, S. and Zohary, T.: *The Eastern Mediterranean, The Biogeo.*, edited by
1090 G. B. Black, K. D. and Shimmiel, Blackwell Publishing, Oxford., 2003.
- 1091 Krom, M. D., Woodward, E. M. S., Herut, B., Kress, N., Carbo, P., Mantoura, R. F. C.,
1092 Spyres, G., Thingstad, T. F., Wassmann, P., Wexels-Riser, C., Kitidis, V., Law, C. S. and
1093 Zodiatis, G.: Nutrient cycling in the south east Levantine basin of the eastern Mediterranean:
1094 Results from a phosphorus starved system, *Deep Sea Res. Part II Top. Stud. Oceanogr.*,
1095 52(22-23), 2879–2896, doi:10.1016/j.dsr2.2005.08.009, 2005.

- 1096 Larnicol, G., Ayoub, N. and Le Traon, P. Y.: Major changes in Mediterranean Sea level
1097 variability from 7 years of TOPEX/Poseidon and ERS-1/2 data, *J. Mar. Syst.*, 33-34, 63–89,
1098 doi:10.1016/S0924-7963(02)00053-2, 2002.
- 1099 Lascaratos, A., Williams, R. G. and Tragou, E.: A mixed-layer study of the formation of
1100 Levantine intermediate water, *J. Geophys. Res.*, 98(C8), 14739, doi:10.1029/93JC00912,
1101 1993.
- 1102 Lascaratos, A., Roether, W., Nittis, K. and Klein, B.: Recent changes in deep water formation
1103 and spreading in the eastern Mediterranean Sea: a review, *Prog. Oceanogr.*, 44(1-3), 5–36,
1104 doi:10.1016/S0079-6611(99)00019-1, 1999.
- 1105 Lehmann, M. F., Bernasconi, S. M., Barbieri, A. and McKenzie, J. A.: Preservation of organic
1106 matter and alteration of its carbon and nitrogen isotope composition during simulated and in
1107 situ early sedimentary diagenesis, *Geochim. Cosmochim. Acta*, 66(20), 3573–3584,
1108 doi:10.1016/S0016-7037(02)00968-7, 2002.
- 1109 Di Leonardo, R., Vizzini, S., Bellanca, A. and Mazzola, A.: Sedimentary record of
1110 anthropogenic contaminants (trace metals and PAHs) and organic matter in a Mediterranean
1111 coastal area (Gulf of Palermo, Italy), *J. Mar. Syst.*, 78(1), 136–145,
1112 doi:10.1016/j.jmarsys.2009.04.004, 2009.
- 1113 Malanotte-Rizzoli, P. and Hecht, A.: Large-scale properties of the eastern mediterranean-A
1114 review, *Oceanol. Acta*, 11(4), 323–335, 1988.
- 1115 Malanotte-Rizzoli, P., Manca, B. B., Alcalá, M. R. D., Bergamasco, A., Bregant, D. and
1116 Georgopoulos, D.: A synthesis of the Ionian Sea hydrography, circulation and water mass
1117 pathways during POEM-Phase I, *Prog. Oceanogr.*, 39(2), 153–204, doi:10.1016/S0079-
1118 6611(97)00013-X, 1997.
- 1119 Manca, B. B., Kovačević, V., Gačić, M. and Viezzoli, D.: Dense water formation in the
1120 Southern Adriatic Sea and spreading into the Ionian Sea in the period 1997–1999, *J. Mar.
1121 Syst.*, 33-34, 133–154, doi:10.1016/S0924-7963(02)00056-8, 2002.
- 1122 Marlowe, I. T., Green, J. C., Neal, A. C., Brassell, S. C., Eglinton, G. and Course, P. A.: Long
1123 chain (n-C37–C39) alkenones in the Prymnesiophyceae. Distribution of alkenones and other
1124 lipids and their taxonomic significance, *Br. Phycol. J.*, 19(3), 203–216,
1125 doi:10.1080/00071618400650221, 1984.
- 1126 Masqué, P., Fabres, J., Canals, M., Sanchez-Cabeza, J. A., Sanchez-Vidal, A., Cacho, I.,
1127 Calafat, A. and Bruach, J. M.: Accumulation rates of major constituents of hemipelagic
1128 sediments in the deep Alboran Sea: a centennial perspective of sedimentary dynamics, *Mar.
1129 Geol.*, 193(3-4), 207–233, doi:10.1016/S0025-3227(02)00593-5, 2003.
- 1130 Mayer, L. M.: Relationships between mineral surfaces and organic carbon concentrations in
1131 soils and sediments, *Chem. Geol.*, 114(3-4), 347–363, doi:10.1016/0009-2541(94)90063-9,
1132 1994.

- 1133 Meador, T. B., Gogou, A., Spyres, G., Herndl, G. J., Krasakopoulou, E., Psarra, S.,
1134 Yokokawa, T., De Corte, D., Zervakis, V. and Repeta, D. J.: Biogeochemical relationships
1135 between ultrafiltered dissolved organic matter and picoplankton activity in the Eastern
1136 Mediterranean Sea, *Deep Sea Res. Part II Top. Stud. Oceanogr.*, 57(16), 1460–1477,
1137 doi:10.1016/j.dsr2.2010.02.015, 2010.
- 1138 Medimap Group: Morpho-bathymetry of the Mediterranean Sea, E: 1=2000000,
1139 CIESM/Ifremer Sp. Publ., Maps and Atlases, two maps (Western Mediterranean and Eastern
1140 Mediterranean), Montecarlo / Brest, Monaco / France., 2007.
- 1141 Meyers, P. A.: Preservation of elemental and isotopic source identification of sedimentary
1142 organic matter, *Chem. Geol.*, 114(3-4), 289–302, doi:10.1016/0009-2541(94)90059-0, 1994.
- 1143 Meyers, P. a.: Organic geochemical proxies of paleoceanographic, paleolimnologic, and
1144 paleoclimatic processes, *Org. Geochem.*, 27(5-6), 213–250, doi:10.1016/S0146-
1145 6380(97)00049-1, 1997.
- 1146 Meyers, P. A. and Arnaboldi, M.: Paleoceanographic implications of nitrogen and organic
1147 carbon isotopic excursions in mid-Pleistocene sapropels from the Tyrrhenian and Levantine
1148 Basins, Mediterranean Sea, *Palaeogeogr. Palaeoclimatol. Palaeoecol.*, 266(1-2), 112–118,
1149 doi:10.1016/j.palaeo.2008.03.018, 2008.
- 1150 Meyers, P. A., Silliman, J. E. and Shaw, T. J.: Effects of turbidity flows on organic matter
1151 accumulation, sulfate reduction, and methane generation in deep-sea sediments on the Iberia
1152 Abyssal Plain, *Org. Geochem.*, 25(1-2), 69–78, doi:10.1016/S0146-6380(96)00106-4, 1996.
- 1153 Milliff, R. F. and Robinson, A. R.: Structure and Dynamics of the Rhodes Gyre System and
1154 Dynamical Interpolation for Estimates of the Mesoscale Variability, *J. Phys. Oceanogr.*,
1155 22(4), 317–337, doi:10.1175/1520-0485(1992)022<0317:SADOTR>2.0.CO;2, 1992.
- 1156 Millot, C. and Taupier-Letage, I.: Additional evidence of LIW entrainment across the
1157 Algerian subbasin by mesoscale eddies and not by a permanent westward flow, *Prog.*
1158 *Oceanogr.*, 66, 231–250, doi:10.1016/j.pcean.2004.03.002, 2005.
- 1159 Mortlock, R. A. and Froelich, P. N.: A simple method for the rapid determination of biogenic
1160 opal in pelagic marine sediments, *Deep Sea Res. Part A. Oceanogr. Res. Pap.*, 36(9), 1415–
1161 1426, doi:10.1016/0198-0149(89)90092-7, 1989.
- 1162 Müller, P. J.: C/N ratios in Pacific deep-sea sediments: Effect of inorganic ammonium and
1163 organic nitrogen compounds sorbed by clays, *Geochim. Cosmochim. Acta*, 41(6), 765–776,
1164 doi:10.1016/0016-7037(77)90047-3, 1977.
- 1165 Nieuwenhuize, J., Maas, Y. E. M. and Middelburg, J. J.: Rapid analysis of organic carbon and
1166 nitrogen in particulate materials, *Mar. Chem.*, 45(3), 217–224, doi:10.1016/0304-
1167 4203(94)90005-1, 1994.
- 1168 Ohkouchi, N., Kawamura, K., Kawahata, H. and Taira, A.: Latitudinal distributions of
1169 terrestrial biomarkers in the sediments from the Central Pacific, *Geochim. Cosmochim. Acta*,
1170 61(9), 1911–1918, doi:10.1016/S0016-7037(97)00040-9, 1997.

- 1171 Olgun, N., Duggen, S., Andronico, D., Kutterolf, S., Croot, P. L., Giammanco, S., Censi, P.
1172 and Randazzo, L.: Possible impacts of volcanic ash emissions of Mount Etna on the primary
1173 productivity in the oligotrophic Mediterranean Sea: Results from nutrient-release experiments
1174 in seawater, *Mar. Chem.*, 152, 32–42, doi:10.1016/j.marchem.2013.04.004, 2013.
- 1175 Orlic, M., Gacic, M. and Laviolette, P. E.: The currents and circulation of the Adriatic Sea,
1176 *Oceanol. Acta*, 15(2), 109–124, 1992.
- 1177 Parinos, C., Gogou, A., Bouloubassi, I., Pedrosa-Pàmies, R., Hatzianestis, I., Sanchez-Vidal,
1178 A., Rousakis, G., Velaoras, D., Krokos, G. and Lykousis, V.: Occurrence, sources and
1179 transport pathways of natural and anthropogenic hydrocarbons in deep-sea sediments of the
1180 eastern Mediterranean Sea, *Biogeosciences*, 10(9), 6069–6089, doi:10.5194/bg-10-6069-
1181 2013, 2013.
- 1182 Pedrosa-Pàmies, R., Sanchez-Vidal, A., Calafat, A., Canals, M. and Durán, R.: Impact of
1183 storm-induced remobilization on grain size distribution and organic carbon content in
1184 sediments from the Blanes Canyon area, NW Mediterranean Sea, *Prog. Oceanogr.*, 118, 122–
1185 136, doi:10.1016/j.pocean.2013.07.023, 2013.
- 1186 Perdue, E. M. and Koprivnjak, J.-F.: Using the C/N ratio to estimate terrigenous inputs of
1187 organic matter to aquatic environments, *Estuar. Coast. Shelf Sci.*, 73(1-2), 65–72,
1188 doi:10.1016/j.ecss.2006.12.021, 2007.
- 1189 Polymenakou, P. N., Tselepides, A., Stephanou, E. G. and Bertilsson, S.: Carbon speciation
1190 and composition of natural microbial communities in polluted and pristine sediments of the
1191 Eastern Mediterranean Sea, *Mar. Pollut. Bull.*, 52(11), 1396–1405,
1192 doi:10.1016/j.marpolbul.2006.03.021, 2006.
- 1193 Psarra, S., Tselepides, A. and Ignatiades, L.: Primary productivity in the oligotrophic Cretan
1194 Sea (NE Mediterranean): seasonal and interannual variability, *Prog. Oceanogr.*, 46(2-4), 187–
1195 204, doi:10.1016/S0079-6611(00)00018-5, 2000.
- 1196 Rabitti, S., Bianchi, F., Boldrin, A., Daros, L., Socal, G. and Totti, C.: Particulate matter and
1197 phytoplankton in the Ionian Sea, *Oceanol. Acta*, 17(3), 297–307, 1994.
- 1198 Rampen, S. W., Willmott, V., Kim, J.-H., Uliana, E., Mollenhauer, G., Schefuß, E., Sinninghe
1199 Damsté, J. S. and Schouten, S.: Long chain 1,13- and 1,15-diols as a potential proxy for
1200 palaeotemperature reconstruction, *Geochim. Cosmochim. Acta*,
1201 doi:10.1016/j.gca.2012.01.024 <<http://dx.doi.org/10.1016/j.gca.2012.01.024>> ,
1202 hdl:10013/epic.40979, 2012.
- 1203 Ratmeyer, V., Balzer, W., Bergametti, G., Chiapello, I., Fischer, G. and Wyputta, U.:
1204 Seasonal impact of mineral dust on deep-ocean particle flux in the eastern subtropical Atlantic
1205 Ocean, *Mar. Geol.*, 159(1-4), 241–252, doi:10.1016/S0025-3227(98)00197-2, 1999.
- 1206 Redfield, A. C., Ketchum, B. H. and Richards, F. A.: The influence of organisms on the
1207 composition of sea-water, in *The Sea*, edited by M. N. Hill, pp. 26–77, Interscience, New
1208 York., 1963.

- 1209 Robinson, A. R., Malanotte-Rizzoli, P., Hecht, A., Michelato, A., Roether, W., Theocharis,
1210 A., Ünlüata, Ü., Pinardi, N., Artegiani, A. and Bergamasco, A.: General circulation of the
1211 Eastern Mediterranean, *Earth-Science Rev.*, 32(4), 285–309, 1992.
- 1212 Robinson, A. R., Leslie, W. G., Theocharis, A. and Lascaratos, A.: Mediterranean Sea
1213 Circulation, in *Encyclopedia of Ocean Sciences*, pp. 1689–1706, Academic Press., 2001.
- 1214 Roether, W. and Well, R.: Oxygen consumption in the Eastern Mediterranean, *Deep Sea Res.*
1215 Part I *Oceanogr. Res. Pap.*, 48(6), 1535–1551, doi:10.1016/S0967-0637(00)00102-3, 2001.
- 1216 Romero, I. C., Schwing, P. T., Brooks, G. R., Larson, R. A., Hastings, D. W., Ellis, G.,
1217 Goddard, E. A. and Hollander, D. J.: Hydrocarbons in Deep-Sea Sediments following the
1218 2010 Deepwater Horizon Blowout in the Northeast Gulf of Mexico, edited by W.-C. Chin,
1219 *PLoS One*, 10(5), e0128371, doi:10.1371/journal.pone.0128371, 2015.
- 1220 Roussiez, V., Ludwig, W., Monaco, A., Probst, J.-L., Bouloubassi, I., Buscail, R. and
1221 Saragoni, G.: Sources and sinks of sediment-bound contaminants in the Gulf of Lions (NW
1222 Mediterranean Sea): A multi-tracer approach, *Cont. Shelf Res.*, 26(16), 1843–1857,
1223 doi:10.1016/j.csr.2006.04.010, 2006.
- 1224 Rullkötter, J.: Organic matter: the driving force for early diagenesis, in *Marine geochemistry*,
1225 edited by H. D. Schulz and M. Zabel, pp. 125–168, Springer Berlin Heidelberg., 2006.
- 1226 Rumolo, P., Barra, M., Gherardi, S., Marsella, E. and Sprovieri, M.: Stable isotopes and C/N
1227 ratios in marine sediments as a tool for discriminating anthropogenic impact., *J. Environ.*
1228 *Monit.*, 13(12), 3399–408, doi:10.1039/c1em10568j, 2011.
- 1229 Rutten, A., de Lange, G. ., Ziveri, P., Thomson, J., Van Santvoort, P. J. M., Colley, S. and
1230 Corselli, C.: Recent terrestrial and carbonate fluxes in the pelagic eastern Mediterranean; a
1231 comparison between sediment trap and surface sediment, *Palaeogeogr. Palaeoclimatol.*
1232 *Palaeoecol.*, 158(3-4), 197–213, doi:10.1016/S0031-0182(00)00050-X, 2000.
- 1233 Salihoğlu, İ., Saydam, C., Baştürk, Ö., Yılmaz, K., Göçmen, D., Hatipoğlu, E. and Yılmaz,
1234 A.: Transport and distribution of nutrients and chlorophyll-a by mesoscale eddies in the
1235 northeastern Mediterranean, *Mar. Chem.*, 29, 375–390, doi:10.1016/0304-4203(90)90024-7,
1236 1990.
- 1237 Sanchez-Vidal, A., Pasqual, C., Kerhervé, P., Calafat, A., Heussner, S., Palanques, a., Durrieu
1238 de Madron, X., Canals, M. and Puig, P.: Impact of dense shelf water cascading on the transfer
1239 of organic matter to the deep western Mediterranean basin, *Geophys. Res. Lett.*, 35(5),
1240 L05605, doi:10.1029/2007GL032825, 2008.
- 1241 Van Santvoort, P. J. M., de Lange, G. J., Thomson, J., Cussen, H., Wilson, T. R. S., Krom, M.
1242 D. and Ströhle, K.: Active post-depositional oxidation of the most recent sapropel (S1) in
1243 sediments of the eastern Mediterranean Sea, *Geochim. Cosmochim. Acta*, 60(21), 4007–4024,
1244 doi:10.1016/S0016-7037(96)00253-0, 1996.

- 1245 Van Santvoort, P. J. M., De Lange, G. J., Thomson, J., Colley, S., Meysman, F. J. R. and
1246 Slomp, C. P.: Oxidation and origin of organic matter in surficial eastern Mediterranean
1247 hemipelagic sediments, *Aquat. Geochemistry*, 8(3), 153–175, 2002.
- 1248 Schlitzer, R.: Ocean Data View, <http://odv.awi.de>, 2011.
- 1249 Schlitzer, R., Roether, W., Oster, H., Junghans, H.-G., Hausmann, M., Johannsen, H. and
1250 Michelato, A.: Chlorofluoromethane and oxygen in the Eastern Mediterranean, *Deep Sea Res.*
1251 *Part A. Oceanogr. Res. Pap.*, 38(12), 1531–1551, doi:10.1016/0198-0149(91)90088-W, 1991.
- 1252 Seiter, K., Hensen, C., Schröter, J. and Zabel, M.: Organic carbon content in surface
1253 sediments—defining regional provinces, *Deep Sea Res. Part I Oceanogr. Res. Pap.*, 51(12),
1254 2001–2026, doi:10.1016/j.dsr.2004.06.014, 2004.
- 1255 Selvaraj, K., Lee, T. Y., Yang, J. Y. T., Canuel, E. A., Huang, J. C., Dai, M., Liu, J. T. and
1256 Kao, S. J.: Stable isotopic and biomarker evidence of terrigenous organic matter export to the
1257 deep sea during tropical storms, *Mar. Geol.*, 364, 32–42, doi:10.1016/j.margeo.2015.03.005,
1258 2015.
- 1259 Siokou-Frangou, I., Gotsis-Skretas, O., Christou, E. D. and Pagou, K.: Plankton
1260 characteristics in the Aegean, Ionian and NW Levantine Seas, in *The Eastern Mediterranean*
1261 *as a Laboratory Basin for the Assessment of Contrasting Ecosystems*, edited by P. Malanotte-
1262 Rizzoli and V. N. Eremeev, pp. 465–473, Kluwer Academic Publisher, Dordrecht, Boston,
1263 London., 1999.
- 1264 Skonieczny, C., Bory, A., Bout-Roumazeilles, V., Abouchami, W., Galer, S. J. G., Crosta, X.,
1265 Diallo, A. and Ndiaye, T.: A three-year time series of mineral dust deposits on the West
1266 African margin: Sedimentological and geochemical signatures and implications for
1267 interpretation of marine paleo-dust records, *Earth Planet. Sci. Lett.*, 364, 145–156,
1268 doi:10.1016/j.epsl.2012.12.039, 2013.
- 1269 Statham, P. J. and Hart, V.: Dissolved iron in the Cretan Sea (eastern Mediterranean), *Limnol.*
1270 *Oceanogr.*, 50(4), 1142–1148, doi:10.4319/lo.2005.50.4.1142, 2005.
- 1271 Stavrakakis, S., Chronis, G., Tselepides, A., Heussner, S., Monaco, A. and Abassi, A.:
1272 Downward fluxes of settling particles in the deep Cretan Sea (NE Mediterranean), *Prog.*
1273 *Oceanogr.*, 46(2-4), 217–240, doi:10.1016/S0079-6611(00)00020-3, 2000.
- 1274 Stavrakakis, S., Gogou, A., Krasakopoulou, E., Karageorgis, A. P., Kontoyiannis, H.,
1275 Rousakis, G., Velaoras, D., Perivoliotis, L., Kambouri, G., Stavrakaki, I. and Lykousis, V.:
1276 Downward fluxes of sinking particulate matter in the deep Ionian Sea (NESTOR site), eastern
1277 Mediterranean: seasonal and interannual variability, *Biogeosciences*, 10(11), 7235–7254,
1278 doi:10.5194/bg-10-7235-2013, 2013.
- 1279 Struck, U., Emeis, K.-C., Voß, M., Krom, M. D. and Rau, G. H.: Biological productivity
1280 during sapropel S5 formation in the Eastern Mediterranean Sea: evidence from stable isotopes
1281 of nitrogen and carbon, *Geochim. Cosmochim. Acta*, 65(19), 3249–3266, doi:10.1016/S0016-
1282 7037(01)00668-8, 2001.

- 1283 Taupier-Letage, I.: On the use of thermal images for circulation studies: applications to the
1284 Eastern Mediterranean basin, in *Remote Sensing of the European Seas*, edited by V. Barale
1285 and M. Gade, pp. 153–164, Springer, Netherlands., 2008.
- 1286 Tesi, T., Miserocchi, S., Goñi, M. A., Langone, L., Boldrin, A. and Turchetto, M.: Organic
1287 matter origin and distribution in suspended particulate materials and surficial sediments from
1288 the western Adriatic Sea (Italy), *Estuar. Coast. Shelf Sci.*, 73(3-4), 431–446,
1289 doi:10.1016/j.ecss.2007.02.008, 2007a.
- 1290 Tesi, T., Miserocchi, S., Goñi, M. A. and Langone, L.: Source, transport and fate of terrestrial
1291 organic carbon on the western Mediterranean Sea, Gulf of Lions, France, *Mar. Chem.*, 105(1-
1292 2), 101–117, doi:10.1016/j.marchem.2007.01.005, 2007b.
- 1293 Tesi, T., Langone, L., Goñi, M. A., Turchetto, M., Miserocchi, S. and Boldrin, A.: Source and
1294 composition of organic matter in the Bari canyon (Italy): Dense water cascading versus
1295 particulate export from the upper ocean, *Deep Sea Res. Part I Oceanogr. Res. Pap.*, 55(7),
1296 813–831, doi:10.1016/j.dsr.2008.03.007, 2008.
- 1297 Theocharis, A., Georgopoulos, D., Lascaratos, A. and Nittis, K.: Water masses and circulation
1298 in the central region of the Eastern Mediterranean: Eastern Ionian, South Aegean and
1299 Northwest Levantine, 1986–1987, *Deep sea Res. part II Top. Stud. Oceanogr.*, 40(6), 1121–
1300 1142, doi:Water masses and circulation in the central region of the Eastern Mediterranean:
1301 Eastern Ionian, South Aegean and Northwest Levantine, 1986–1987, 1993.
- 1302 Theocharis, A., Balopoulos, E., Kioroglou, S., Kontoyiannis, H. and Iona, A.: A synthesis of
1303 the circulation and hydrography of the South Aegean Sea and the Straits of the Cretan Arc
1304 (March 1994–January 1995), *Prog. Oceanogr.*, 44(4), 469–509, doi:10.1016/S0079-
1305 6611(99)00041-5, 1999.
- 1306 Theodosi, C., Parinos, C., Gogou, A., Kokotos, a., Stavrakakis, S., Lykousis, V., Hatzianestis,
1307 J. and Mihalopoulos, N.: Downward fluxes of elemental carbon, metals and polycyclic
1308 aromatic hydrocarbons in settling particles from the deep Ionian Sea (NESTOR site), Eastern
1309 Mediterranean, *Biogeosciences*, 10(7), 4449–4464, doi:10.5194/bg-10-4449-2013, 2013.
- 1310 Thingstad, T. F., Krom, M. D., Mantoura, R. F. C., Flaten, G. A. F., Groom, S., Herut, B.,
1311 Kress, N., Law, C. S., Pasternak, A., Pitta, P., Psarra, S., Rassoulzadegan, F., Tanaka, T.,
1312 Tselepidis, A., Wassmann, P., Woodward, E. M. S., Riser, C. W., Zodiatis, G. and Zohary,
1313 T.: Nature of phosphorus limitation in the ultraoligotrophic eastern Mediterranean., *Science*,
1314 309(5737), 1068–71, doi:10.1126/science.1112632, 2005.
- 1315 Triantaphyllou, M. V.: Coccolithophore export production and response to seasonal surface
1316 water variability in the oligotrophic Cretan Sea (NE Mediterranean), *Micropaleontology*,
1317 50(Suppl_1), 127–144, doi:10.2113/50.Suppl_1.127, 2004.
- 1318 Tsapakis, M. and Stephanou, E. G.: Occurrence of gaseous and particulate polycyclic
1319 aromatic hydrocarbons in the urban atmosphere: study of sources and ambient temperature
1320 effect on the gas/particle concentration and distribution, *Environ. Pollut.*, 133(1), 147–156,
1321 doi:10.1016/j.envpol.2004.05.012, 2005.

- 1322 Turchetto, M., Boldrin, A., Langone, L., Misericocchi, S., Tesi, T. and Foglini, F.: Particle
1323 transport in the Bari Canyon (southern Adriatic Sea), *Mar. Geol.*, 246(2-4), 231–247,
1324 doi:10.1016/j.margeo.2007.02.007, 2007.
- 1325 UNEP/MAP/MEDPOL: Sub-regional assessment of the Status of Marine and Coastal
1326 Ecosystems and of Pressures to the Marine and Coastal Environment Eastern Mediterranean
1327 Sea UNEP(DEPI)/MED WG.350/Inf.4, pp. 37–38, Barcelona., 2010.
- 1328 Ursella, L., Kovačević, V. and Gačić, M.: Tidal variability of the motion in the Strait of
1329 Otranto, *Ocean Sci.*, 10(1), 49–67, doi:10.5194/os-10-49-2014, 2014.
- 1330 Volkman, J. K.: A review of sterol markers for marine and terrigenous organic matter, *Org.*
1331 *Geochem.*, 9(2), 83–99, doi:10.1016/0146-6380(86)90089-6, 1986.
- 1332 Volkman, J. K.: Lipid markers for marine organic matter, in *Marine Organic Matter:*
1333 *Biomarkers, Isotopes and DNA*, edited by J. K. Volkman, pp. 27–70, Springer Verlag,
1334 Berlin., 2006.
- 1335 Volkman, J. K., Kearney, P. and Jeffrey, S. W.: A new source of 4-methyl sterols and 5 α (H)-
1336 stanols in sediments: prymnesiophyte microalgae of the genus *Pavlova*, *Org. Geochem.*,
1337 15(5), 489–497, doi:10.1016/0146-6380(90)90094-G, 1990.
- 1338 Volkman, J. K., Barrett, S. M. and Blackburn, S. I.: Eustigmatophyte microalgae are potential
1339 sources of C29 sterols, C22-C28 n-alcohols and C28-C32 n-alkyl diols in freshwater
1340 environments, *Org. Geochem.*, 30(5), 307–318, doi:10.1016/S0146-6380(99)00009-1, 1999.
- 1341 Wang, Z., Fingas, M. and Page, D. S.: Oil spill identification, *J. Chromatogr. A*, 843(1-2),
1342 369–411, doi:10.1016/S0021-9673(99)00120-X, 1999.
- 1343 Weldeab, S., Emeis, K.-C., Hemleben, C. and Siebel, W.: Provenance of lithogenic surface
1344 sediments and pathways of riverine suspended matter in the Eastern Mediterranean Sea:
1345 evidence from $^{143}\text{Nd}/^{144}\text{Nd}$ and $^{87}\text{Sr}/^{86}\text{Sr}$ ratios, *Chem. Geol.*, 186(1-2), 139–149,
1346 doi:10.1016/S0009-2541(01)00415-6, 2002.
- 1347 Ziveri, P., Rutten, A., de Lange, G. ., Thomson, J. and Corselli, C.: Present-day coccolith
1348 fluxes recorded in central eastern Mediterranean sediment traps and surface sediments,
1349 *Palaeogeogr. Palaeoclimatol. Palaeoecol.*, 158(3-4), 175–195, doi:10.1016/S0031-
1350 0182(00)00049-3, 2000.
- 1351 Zoccolotti, L. and Salusti, E.: Observations of a vein of very dense marine water in the
1352 southern Adriatic Sea, *Cont. Shelf Res.*, 7(6), 535–551, doi:10.1016/0278-4343(87)90020-3,
1353 1987.
- 1354

1356 Table 1. Location, depth and collection date of sediment samples.

Sample Code	Latitude (N)	Longitude (E)	Water depth (m)	Date of collection	Physiographic regions
Ionian Sea					
<i>North</i>					
H12	39.30	19.30	1450	Jan-07	Otranto Valley
H07	39.11	17.75	1866	Jan-07	Taranto Valley
<i>Central</i>					
BF27	38.22	16.63	1264	juny-09	Calabrian Slope
BF13	37.66	16.56	2012	juny-09	Calabrian Arc
BF15	36.20	16.35	3335	juny-09	Ionian Basin
H04	35.92	16.00	3750	Jan-07	Ionian Basin
<i>West</i>					
H02	35.75	21.00	3008	Jan-07	Ionian Basin
H05	37.50	18.50	3154	Jan-07	Ionian Basin
H03	35.70	18.50	4087	Jan-07	Ionian Basin
S. Aegean Sea (Cretan Sea)					
Red5	35.68	25.10	1018	May-10	Cretan Trough
Red9	36.00	23.89	1200	May-11	Cretan Trough
Red4	35.76	25.10	1615	May-10	Cretan Trough
Red8	36.07	25.28	1715	May-11	Cretan Trough
W Cretan Straits					
H01	35.70	23.00	2117	Jan-07	Kithira Strait
Red3	35.40	23.40	2976	May-10	Antikithira Strait
Red3.1	35.30	23.32	3317	May-10	Antikithira Strait
Red7	34.60	24.15	3589	May-11	Ptolemy Strait
NW Levantine Sea					
<i>Ierapetra Basin</i>					
Red13	34.95	25.93	1101	juny-12	Cretan-Rhodes Ridge
BF19	34.51	25.76	1200	juny-09	Hellenic Trench
BF22	34.48	25.87	2015	juny-09	Hellenic Trench
Red15.1	34.61	25.92	2428	juny-12	Hellenic Trench
Red1.1	34.40	26.25	3568	juny-12	Hellenic Trench
Ier01	34.44	26.19	3626	Jan-07	Hellenic Trench
<i>Open Sea</i>					
Rho02	35.62	27.70	1305	Jan-07	Rhodes Strait
Her01	33.92	27.74	2680	Jan-07	EM Ridge
Red2	33.74	26.15	2717	May-10	EM Ridge
Red2.1	33.71	26.34	2720	May-10	EM Ridge
BF24	34.15	25.57	2902	juny-09	Pliny Trench
Her03	33.67	29.00	3090	Jan-07	Herodotus Basin

January 2007 samples were collected during the M71 (Leg 3) cruise onboard the *R/V Meteor* (University of Hamburg, Germany), June 2009 samples during the Biofun1 cruise onboard the *R/V Sarmiento de Gamboa* (CSIC-UB, Spain), and May 2010, 2011 and June 2012 samples during the ReDEco cruises onboard the *R/V Aegaeo* (HCMR, Greece).

Table 2. Bulk composition and sedimentological parameters of the investigated surface sediments.

Sample Code	Clay _{bulk} (% ,<4 μm)	Silt _{bulk} (%, 4-63 μm)	Sand _{bulk} (%, 63 μm-2 mm)	Sorting _{bulk}	Sorting _{litho}	Skewnes _{bulk}	D ₅₀ bulk (μm)	Lithogenic (%)	CaCO ₃ (%)	Opal (%)	OC (%)	TN/OC	δ ¹³ C (‰)	OC _{mar} (%)	OC _{terr} (%)
Ionian Sea															
<i>North</i>															
H12	18.1	76.7	5.24	3.47	3.31	-0.13	14.6	71.2	28.5	0.03	0.15	0.08	-24.2	42.3	57.7
H07	41.2	58.8	0.00	3.01	4.12	-0.07	5.34	75.7	22.0		1.15	0.08	-24.4	40.2	59.8
<i>Central</i>															
BF27	52.8	46.1	1.04	3.38	2.83	-0.04	3.97	80.8	17.8	0.16	0.64	0.12	-23.0	60.0	40.0
BF13	50.8	48.1	1.08	3.41	2.92	-0.05	4.17	76.7	22.0	0.21	0.58	0.12	-22.9	62.7	37.3
BF15	39.1	57.0	3.98	4.01	2.91	0.03	5.88	77.9	21.6		0.28	0.14	-22.5	68.8	31.2
H04	41.6	58.4	0.04	4.69	3.53	-0.23	5.52	85.4	13.2	0.04	0.65	0.13	-23.6	50.9	49.1
<i>West</i>															
H02	53.3	46.7	0.00	2.99	6.16	-0.07	3.92	47.7	51.3	0.04	0.45	0.10	-22.5	68.6	31.4
H05	41.6	58.4	0.00	2.98	3.48	-0.01	5.34	60.7	38.2		0.57	0.11	-23.7	50.2	49.8
H03	34.5	65.5	0.08	3.11	3.49	-0.04	7.03	77.6	21.0	0.11	0.63	0.10	-24.6	35.8	64.2
S. Aegean Sea (Cretan Sea)															
Red5	54.0	46.0	0.00	3.32	3.61	-0.01	3.88	32.5	66.5	0.24	0.39	0.10	-22.4	69.2	30.8
Red9	50.1	49.9	0.00	3.24	3.28	-0.01	4.23	46.6	52.2	0.15	0.55	0.12	-22.6	67.4	32.6
Red4	52.6	47.4	0.00	3.26	3.58	-0.06	4.00	39.3	59.8	0.09	0.42	0.12	-22.2	73.0	27.0
Red8	53.1	46.9	0.00	3.12	3.36	-0.03	3.97	44.0	55.3	0.08	0.33	0.15	-22.0	75.5	24.5
W Cretan Straits															
H01	55.1	44.9	0.00	4.74	4.77	-0.11	3.65	42.8	56.6		0.29	0.12	-22.6	66.5	33.5
Red3	14.5	37.9	47.7	5.23	4.54	-0.45	56.6	59.2	39.9	0.15	0.37	0.08	-18.3		
Red3.1	37.7	61.5	0.88	4.32	3.82	-0.07	6.74	55.7	43.0	0.12	0.58	0.09	-22.9	62.4	37.6
Red7	36.0	63.5	0.59	3.55	3.57	-0.01	6.37	61.4	37.5	0.07	0.51	0.12	-22.7	64.7	35.3
NW Levantine Sea															
<i>Ierapetra Basin</i>															
Red13	50.1	49.3	0.66	4.84	3.07	-0.15	4.23	59.1	39.8	0.22	0.46	0.11	-22.3	71.1	28.9
BF19	51.1	38.5	10.4	4.98	3.43	0.27	4.12	39.4	59.9		0.34	0.14	-22.6	67.3	32.7
BF22	47.5	44.0	8.53	4.71	3.34	0.20	4.56	57.7	41.7		0.26	0.15	-21.2	87.7	12.3
Red15.1	47.5	51.8	0.73	4.60	2.77	-0.03	4.59	51.8	46.9	0.80	0.61	0.08	-23.3	56.1	43.9
Red1.1	57.1	42.8	0.15	3.73	2.61	-0.13	3.53	51.8	47.1	0.05	0.54	0.10	-21.5	83.8	16.2
Ier01	49.1	50.4	0.00	3.84	2.67	0.03	4.35	55.6	43.3	0.06	0.52	0.12	-21.7	80.2	19.8
<i>Open Sea</i>															
Rho02	43.0	55.9	1.11	4.43	3.25	-0.14	5.24	58.4	40.6	0.16	0.47	0.12	-22.7	65.2	34.8
Her01	48.2	51.8	0.00	3.88	4.89	0.04	4.44	35.8	63.4	0.13	0.31	0.15	-22.7	65.5	34.5
Red2	32.4	53.2	14.4	4.95	3.85	-0.01	11.1	45.0	53.9	0.07	0.5	0.09	-24.0	46.2	53.8
Red2.1	48.7	51.1	0.21	4.30	3.92	0.11	4.42	44.2	55.0	0.10	0.37	0.11	-22.4	70.5	29.5
BF24	43.1	45.0	11.9	5.25	3.51	0.20	5.34	55.0	44.3	0.11	0.29	0.16	-22.3	70.6	29.4
Her03	39.8	60.2	0.00	4.05	3.20	-0.19	5.81	48.2	50.7	0.11	0.49	0.11	-22.4	70.2	29.8

*empty cell = not determined

1365 **Table 3.** Concentrations (OC-normalized) and indices of the considered lipid biomarkers.

Station	Σ TerNA ^a ($\mu\text{g g}^{-1}$ OC)	Σ TerN-OH ($\mu\text{g g}^{-1}$ OC)	Σ Mar ($\mu\text{g g}^{-1}$ OC)	Σ Alkenones ^b ($\mu\text{g g}^{-1}$ OC)	Σ C ₃₀ diols&keto-ols ^c ($\mu\text{g g}^{-1}$ OC)	Σ Sterols ^d ($\mu\text{g g}^{-1}$ OC)	$_{27}\Delta^5$ ($\mu\text{g g}^{-1}$ OC)	$_{28}\Delta^{5,22}$ ($\mu\text{g g}^{-1}$ OC)	$_{29}\Delta^5$ ($\mu\text{g g}^{-1}$ OC)	$_{30}\Delta^{22}$ ($\mu\text{g g}^{-1}$ OC)	CPI _{NA} ^a	CPI _{N-OH}	[NA]/ [N-OH]
Ionian Sea													
<i>North</i>													
H12	54.9	19.0	29.4	6.75	14.7	62.4	29.7	3.22	24.8	4.72	4.14	4.00	2.90
H07	40.8	13.4	34.5	5.97	14.6	35.6	6.77	5.52	14.9	8.37	4.39	4.14	3.03
<i>Central</i>													
BF27													
BF13													
BF15													
H04	169	52.1	54.1	12.3	21.5	59.6	10.6	8.57	28.6	11.7	4.04	5.95	3.24
<i>West</i>													
H02	176	35.2	34.2	8.14	19.7	17.1	3.67	2.36	7.06	3.96	3.57	3.73	5.00
H05	211	42.8	47.2	12.5	25.0	24.2	4.12	3.43	10.4	6.28	4.07	3.63	4.93
H03	214	37.0	35.7	8.77	17.4	25.2	6.04	3.65	9.62	5.92	2.80	4.08	5.78
S. Aegean Sea (Cretan Sea)													
Red5	206	50.7	45.3	20.1	15.9	40.1	10.8	4.74	20.0	4.51	5.07	4.89	4.06
Red9	101	14.7	22.2	9.85	7.30	17.7	3.77	2.66	8.83	2.42	7.25	5.12	6.88
Red4	196	48.4	41.0	17.4	14.8	38.6	11.5	4.63	18.3	4.15	5.36	5.21	4.05
Red8	127	29.4	35.5	16.8	12.3	26.3	5.62	3.23	14.2	3.20	6.40	4.97	4.32
W Cretan Straits													
H01	127	26.2	18.2	3.41	11.3	10.3	2.22	1.35	4.55	2.22	6.64	6.13	4.84
Red3	120	30.4	70.1	21.2	28.1	34.4	7.85	9.33	5.79	11.4	2.90	4.27	3.93
Red3.1	218	50.0	29.0	10.8	11.8	20.7	3.87	3.15	10.4	3.30	3.63	4.02	4.37
Red7	184	43.7	59.2	30.5	19.4	28.6	6.17	3.61	13.1	5.69	3.99	4.63	4.21
NW Levantine Sea													
<i>Ierapetra Basin</i>													
Red13	156	36.8	38.8	14.1	16.1	34.5	10.2	4.97	15.8	3.60	7.95	5.82	4.24
BF19													
BF22													
Red15.1	126	28.3	32.6	11.5	14.1	21.3	4.20	3.21	10.1	3.88	5.26	5.03	4.44
Red1.1	166	38.6	36.9	14.1	14.7	23.9	5.14	3.67	10.7	4.39	6.07	4.79	4.30
Ier01	206	44.4	59.0	11.1	35.0	29.8	4.94	4.69	11.9	8.30	6.37	3.68	4.63
<i>Open Sea</i>													
Rho02	166	49.9	51.2	5.92	33.2	30.2	5.56	4.90	12.6	7.17	6.88	4.68	3.33
Her01	195	52.2	66.3	14.2	35.8	46.5	11.3	7.59	18.9	8.71	4.43	3.70	3.74
Red2													
Red2.1	483	105	72.6	23.6	35.5	47.8	7.86	6.54	26.4	6.97	1.93	4.23	4.59
BF24													
Her03	157	39.7	45.7	7.95	29.5	22.2	4.57	3.05	9.39	5.23	3.69	3.49	3.96

*empty cell = not determined

^a reported by Parinos et al., 2013^b Sum of the concentrations of C37:3M, C37:2M, C36:2FAME, C38:3Et, C38:3M, C38:2Et, C38:2M (the corresponding unsaturated homologues are indicated with the number of their carbon atoms (n) and the number of double bonds (x)-(Cn:x); M: methyl; Et: Ethyl; FAME: Fatty acid methyl ester).^c Sum of the concentrations of long-chain C₃₀ n-alkan-1,15-diols and C₃₀ keto-ols^d Sum of the major C₂₇-C₃₀ sterols considered in this study i.e., cholesterol (cholest-5-en-3 β -ol; $_{27}\Delta^5$), brassicasterol (24-methylcholesta-5,22-dien-3 β -ol; $_{28}\Delta^{5,22}$), β -sitosterol (24-ethylcholesta-5-en-3 β -ol; $_{29}\Delta^5$) and dinosterol (4 α ,23,24-trimethyl-5 α (H)-cholest-22(E)-en-3 β -ol - $_{30}\Delta^{22}$)

1367 **Figure captions**

1368 **Fig. 1.** (a) Location of sampling sites across the open Eastern Mediterranean
1369 Sea (see also Table 1). The map was produced using GEBCO Digital Atlas
1370 (IOC, IHO and BODC, 2003). (b) Plot of longitude vs. water depth of sampling
1371 stations.

1372 **Fig. 2.** Statistical dendrogram of type-averaged grain-size profiles and
1373 geographical distribution of grain-size compositional types for a) the lithogenic
1374 fraction and b) the bulk fraction of the investigated sediments.

1375 **Fig. 3.** Spatial distribution of (a) lithogenics, (b) CaCO₃ contents, (c) OC
1376 contents, (d) molar TN/OC ratios, and (e) δ¹³C values in surface sediments of
1377 the deep Eastern Mediterranean Sea.

1378 **Fig. 4.** Spatial distributions of the OC-normalized concentrations of (a)
1379 Unresolved Complex Mixture (UCM), (b) ΣTerNA, (c) ΣTerN-OH and (d) ΣMar
1380 in surface sediments of the deep Eastern Mediterranean Sea. Abbreviations of
1381 lipid biomarkers are defined in the text.

1382 **Fig. 5.** (a) Scatter plot of the factor loadings of the three principal components
1383 obtained in the Principal Component Analysis, and (b) plot of the scores found
1384 at each station. Abbreviations of lipid biomarkers are defined in the text.

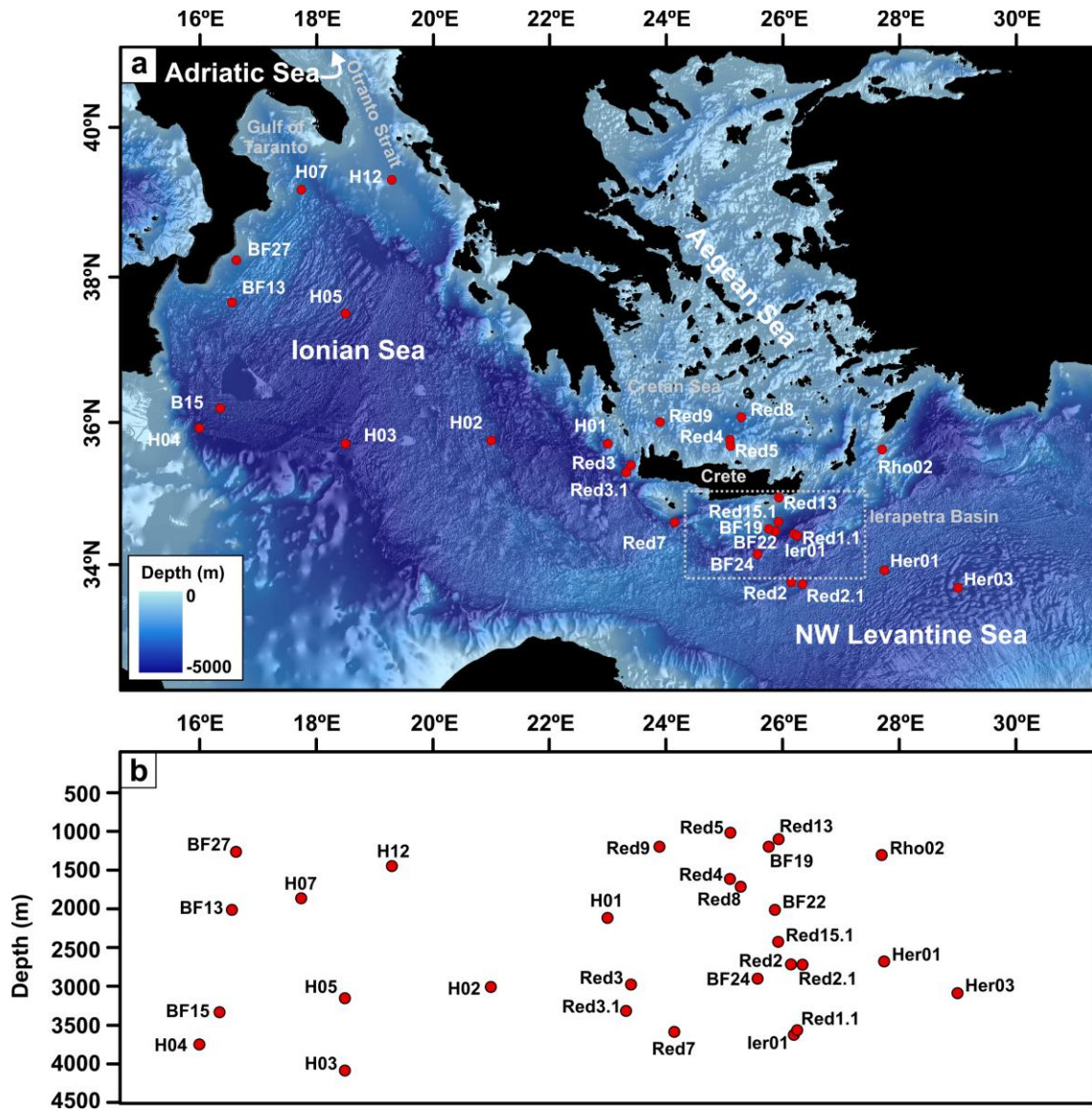
1385 **Fig. 6.** (a) Co-plot of the weight percent content of nitrogen (TN) vs. organic
1386 carbon (OC) for the deep-sea surface sediments analysed. The linear fit of the
1387 data is shown (dotted line) along with the Redfield ratio N₁₆/C₁₀₆ associated with
1388 the fresh marine phytoplankton (0.17 wt. /wt.). (b) Plot of molar TN/OC ratios vs.
1389 δ¹³C, in surface sediments of the deep Eastern Mediterranean Sea. The
1390 compositional ranges of organic matter sources illustrated in plots (boxes)
1391 derive from previously published studies (see section 5.1).

1392 **Fig. 7.** Distribution of OC content and bulk sediment tracers (TN/OC and δ¹³C)
1393 in surface sediments of the deep Eastern Mediterranean Sea. The histogram
1394 reflects a spatially variable mixture of marine and terrestrial sources for
1395 sedimentary OM. Orange triangles and green circles correspond to molar
1396 TN/OC ratios and δ¹³C values, respectively.

1397 **Fig. 8.** Spatial distribution of lipid biomarker indices (a) [NA]/[N-OH], (b) CPI_{NA}
1398 and (c) CPI_{N-OH}. Abbreviations of lipid biomarker indices are defined in the text.

1399

1400 1.



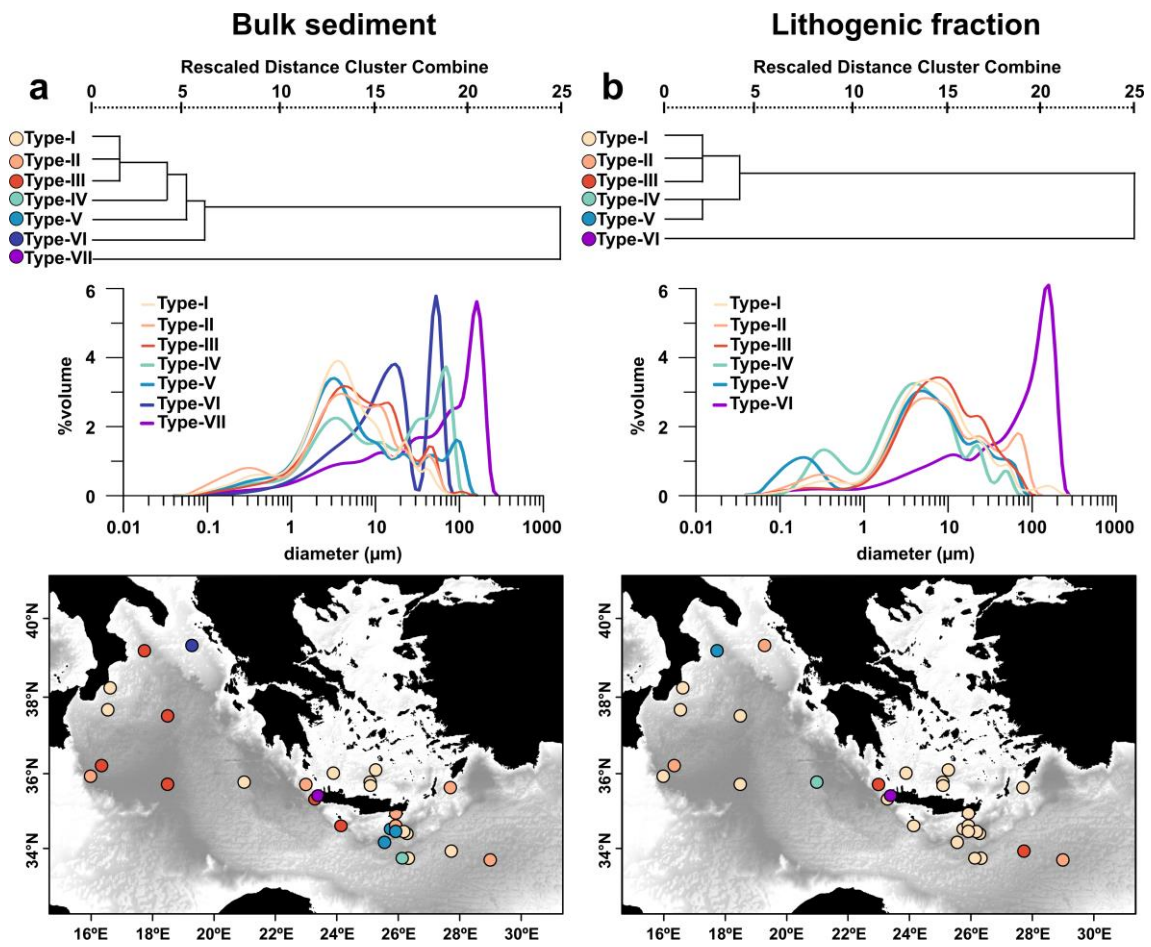
1401

1402

1403

1404

1405

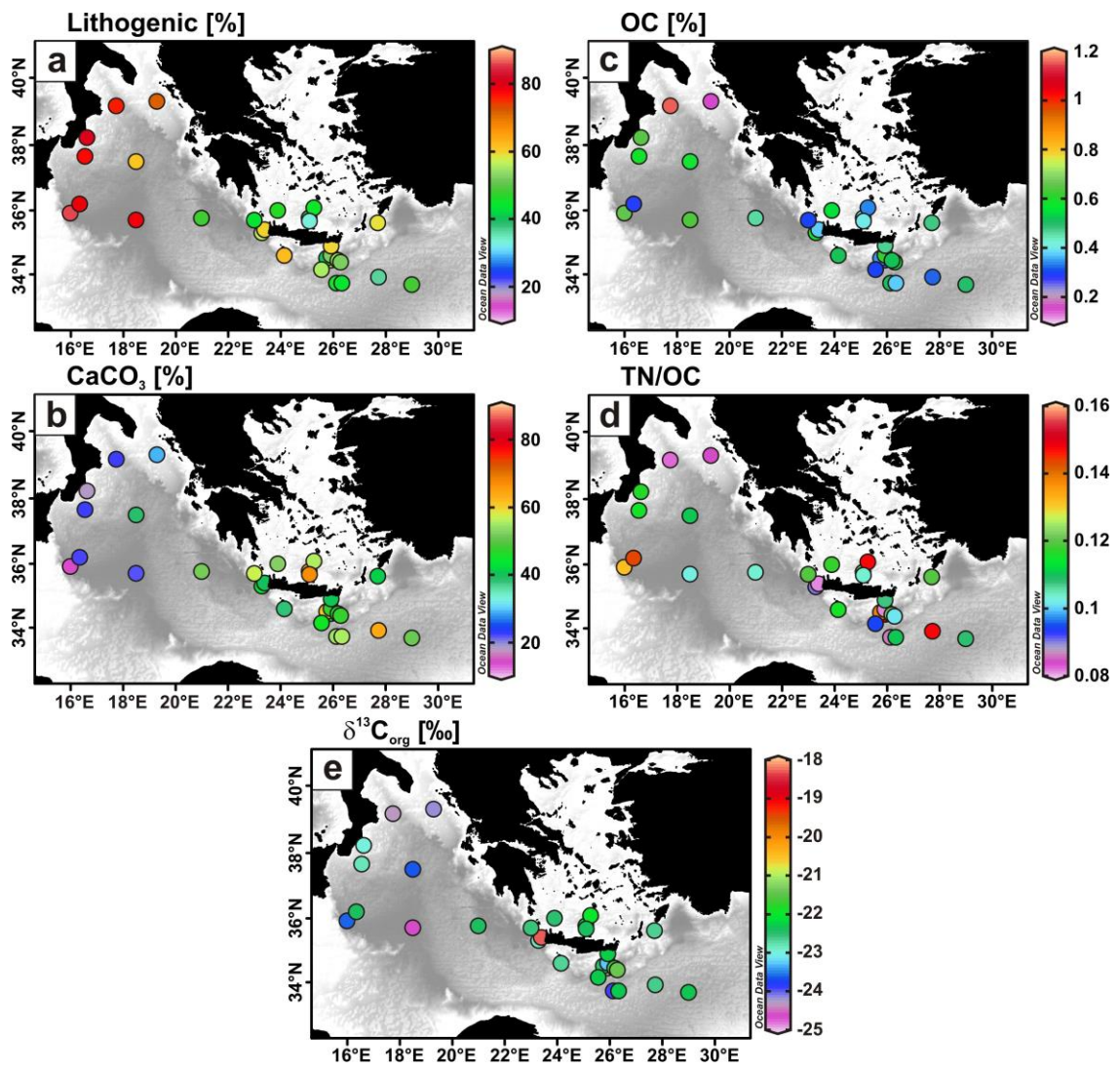


1407

1408

1409

1410



1412

1413

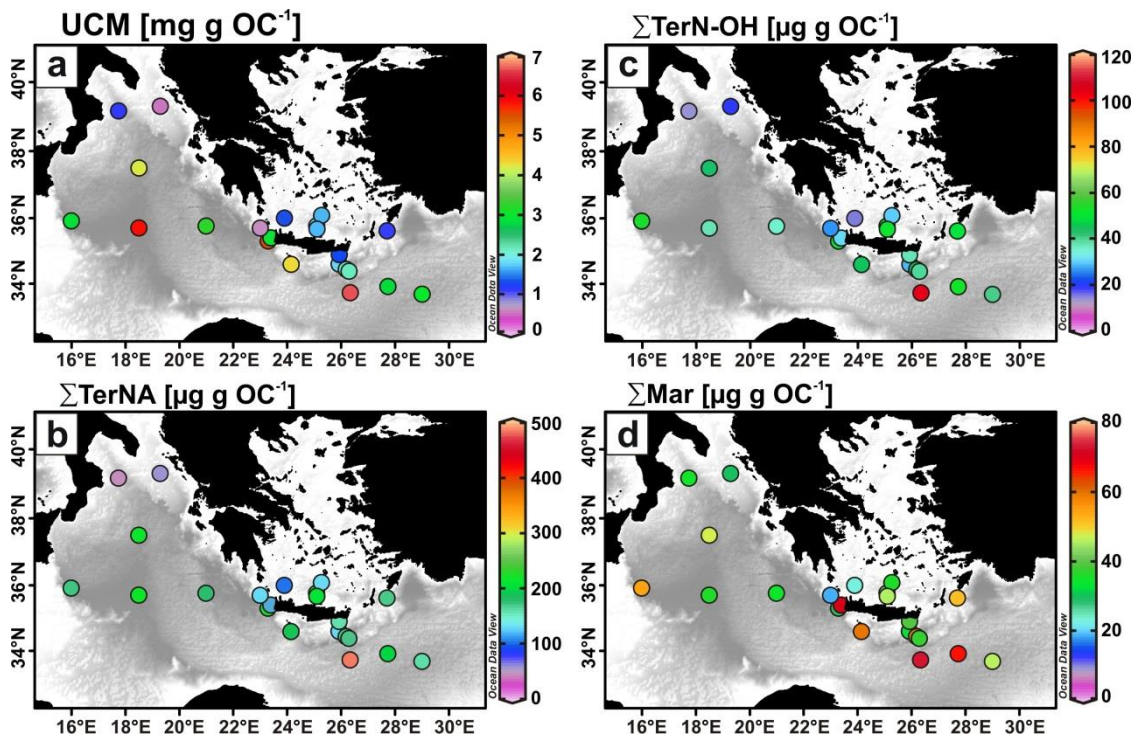
1414

1415

1416

1417 4.

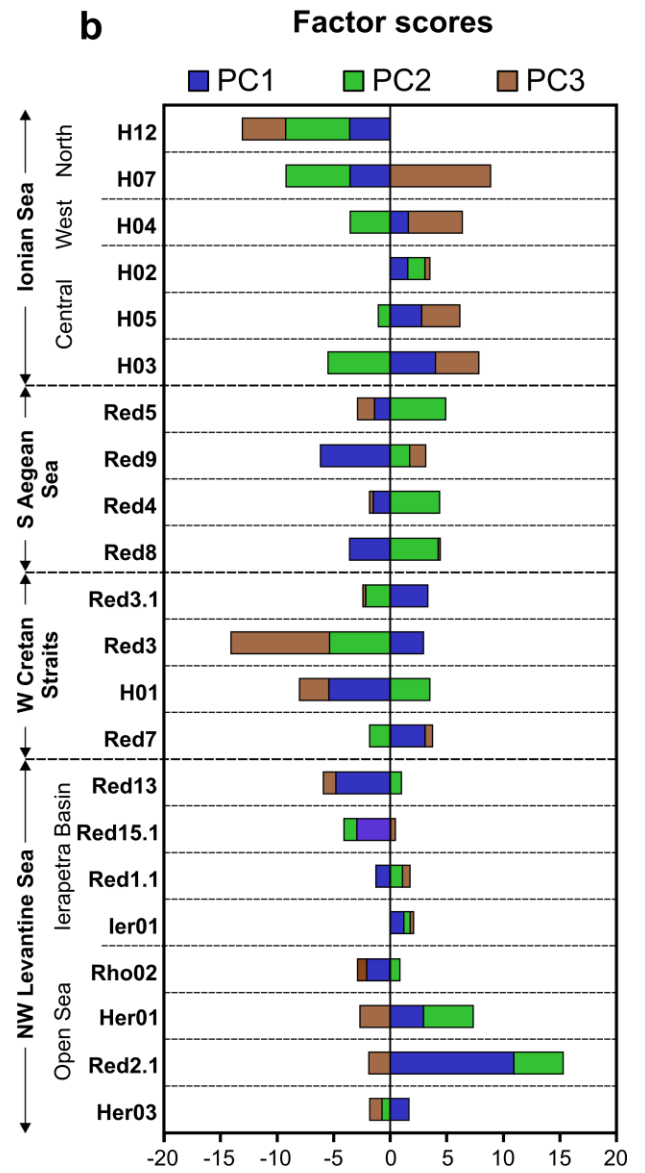
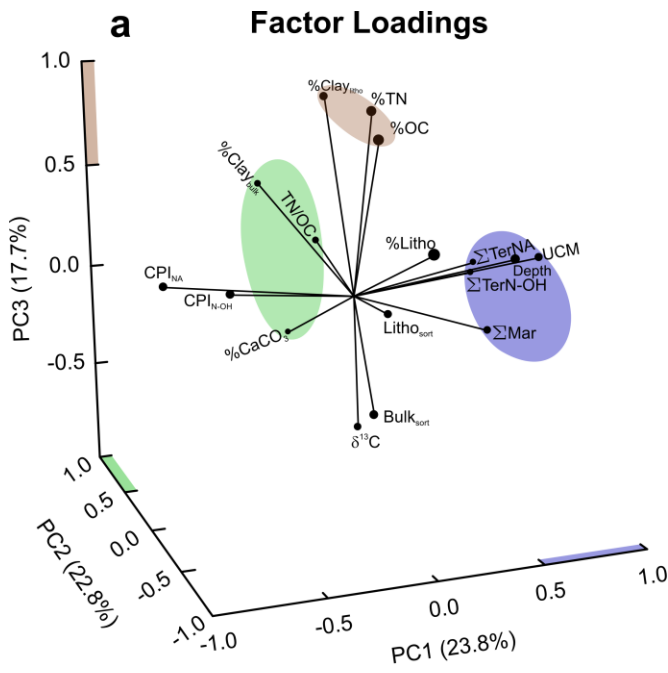
1418

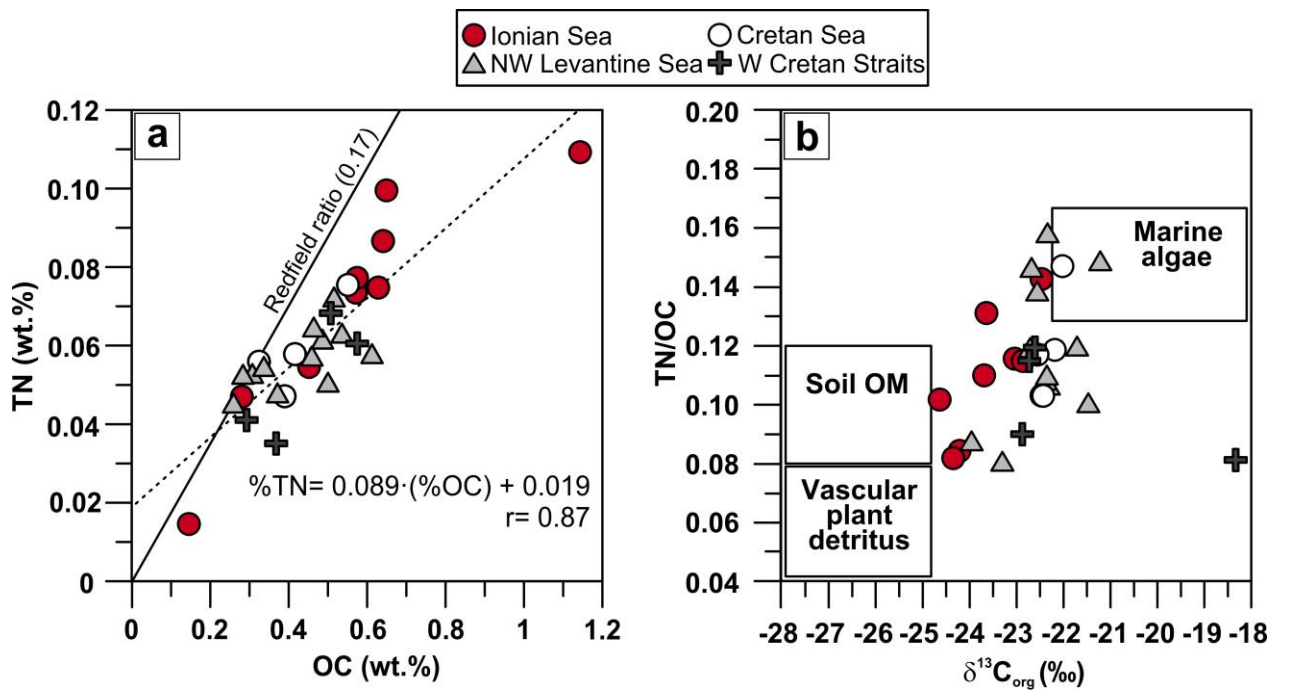


1419

1420

1421



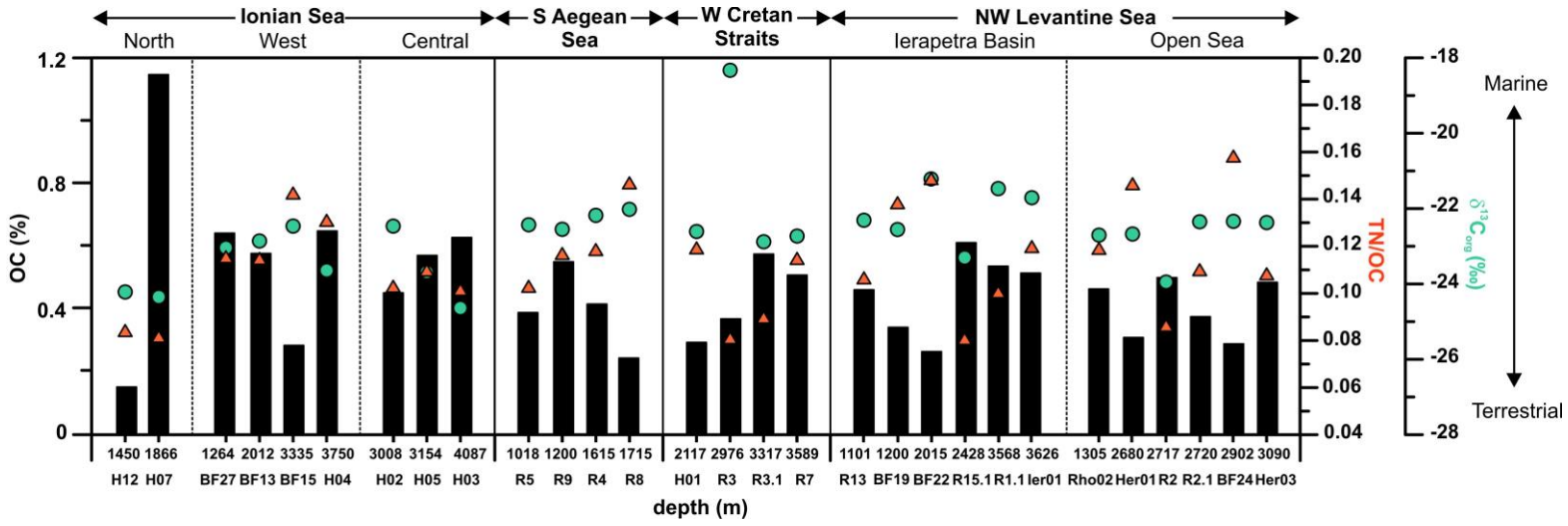


1426

1427

1428 7.

1429



1430

1431

1432

